indicates the possibility that epigenetic modifications could generate a significant magnitude to induce the sensitivity to differentiation induction and chemotherapy reagents in GI cancer. Nevertheless, long-term behavior of iPC cells with deleterious mutations remains to be studied. Furthermore, safety issues involved in synthesizing tumor-producing iPS cells from non-cancerous somatic cells should be addressed to avoid an unexpected malignant transformation in the course of medical innervations in human diseases.

In the present study, we introduced defined factors in three GI cancer cell lines to establish short-term cultured (Sc)-iPC cells, similar to iPS/iPC cells production [3,4], which were cultured to assess long-term cultured (Lc)-iPC cells. The aggressive phenotype was observed in a cell line with genetic mutations, which were associated with endogenous *c-MYC* activation.

2. Materials and methods

For detailed information see Supplementary Information.

2.1. Cell culture

Three GI cell lines were maintained in DMEM (Sigma, St. Louis, MO) containing 10% fetal bovine serum (FBS) at 37 °C in a 5% humidified CO_2 atmosphere, and used for reprogramming. Colorectal cancer DLD-1 and hepatocellular carcinoma PLC/PRF/5 (PLC) cells were purchased from the Japanese Cancer Research Resources Bank (Tokyo, Japan), and cholangiocellular carcinoma HuCC-T1 cells were a gift from Dr. Gregory J. Gores. PLAT-E cells (Cell Biolabs, San Diego, CA) were maintained in DMEM containing 10% FBS, 1 μg/ml puromycin (Sigma), and 10 μg/ml blasticidin (Sigma). 293FT (Invitrogen, Carlsbad, CA) cells were maintained in DMEM containing 10% FBS and 500 μg/ml geneticin (Invitrogen). The medium was replaced every 2 or 3 days.

2.2. Transfection and Sc-iPC cells production

293FT cells were used to produce the lentiviral vector harboring the mouse retroviral receptor by introducing the pLenti6/UbC/mSlc7a1 plasmid (Addgene Cambridge, MA). After transfection, the lentivirus was purified by filtration. Cancer cells transfected using the lentivirus mSlc7a1, as described above, were infected with retroviruses in the medium. Retroviral vectors were produced by transfecting constructed plasmids into PLAT-E cells, and the culture medium was purified by filtration, concentrated, and used for infection.

Eight days after transduction, the transfected cells in 10% FBS–DMEM were harvested and re-plated on culture plates coated with Matrigel hESC-qualified Matrix (BD Biosciences, Bedford, MA). The medium was replaced the next day with mTeSR1 medium (StemCell Technologies, Vancouver, BC, Canada). Post-Sc-iPC production was induced as described previously [4]. Post-Sc-iPC cells were cultured for an additional 10 weeks in 10% FBS–DMEM primary culture medium until day 90 to induce Lc-iPC cells.

2.3. Quantitative reverse transcription (RT)-PCR

Total RNA was extracted, reverse transcribed, and subjected to quantitative real-time RT-PCR using the LightCycler TaqMan Master kit (Roche Diagnostics GmbH, Mannheim, Germany) and the LightCycler FastStart DNA Master SYBR Green I kit (Roche).

2.4. Immunofluorescence staining

Cells were fixed in 4% paraformaldehyde, immunostained with specific antibodies, and visualized by fluorescence microscopy (BZ-8000; Keyence, Osaka, Japan). For adipogenic or osteogenic differentiation, iPC cells were treated with the supplements (R&D Systems, Minneapolis, MN) in culture medium for 2 weeks.

2.5. Chromatin immunoprecipitation assay

Cells were cross-linked with 1% formaldehyde, immunoprecipitated using the anti-trimethyl lysine 4 histone H3 antibody (Nippon Gene, Toyama, Japan), and used for semi-quantitative PCR.

2.6. Invasion and chemosensitivity assay

Cell invasion was assessed using a CytoSelect Cell Invasion Assay kit (Cell Biolabs) with or without 100 nM retinol (RA; Sigma) or 10 nM 1,25-dihydroxy-vitamin D3 (VD3; Sigma) treatment. The *in vitro* chemotherapeutic sensitivity to 5-fluorouracil (5-FU; Kyowa Hakkou, Tokyo, Japan) was assessed by the 3-(4-,5-dimethylthiazol-2-yl)-2,5-diphenyltetrazolium bromide (MTT; Sigma) assay.

2.7. In vivo tumorigenicity assay

In vivo tumorigenicity was evaluated by transplanting cells into immunodeficient NOD.CB17-Prkdcscid/J (NOD-scid) mice (Charles Liver, Yokohama, Japan). Eight weeks after injection, tumors were dissected, measured, and fixed with 4% paraformaldehyde. Paraffin-embedded tissue was sliced, stained with hematoxylin–eosin (HE), and subjected to immunohistochemistry using the anti-c-Myc antibody.

3. Results

3.1. Introduction of defined ES-like transcriptional factors elicited an immature state in cancer cells

The experimental schedule is shown in Fig. 1A. Four defined factors, *c-MYC*, *SOX2*, *OCT3/4*, and *KLF4*, were transfected into three cancer cell lines, HuCC-T1, PLC, and DLD-1, using the retroviral packaging cell line PLAT-E at day 0. Cells were trypsinized, harvested, and re-plated onto Matrigel-coated plates at day 8 after transfection. The next day, culture dishes were replaced with human ES cell culture medium (mTeSR1). Three weeks after transduction, round-shaped, colonies, which were distinct from background cells, started appearing. The colonies were picked up at day 30 (Supplementary Fig. S1) and *NANOG* expression was confirmed using fluorescence microscopic observation for green fluorescent protein (*Gfp*) expression after transiently transfecting the *NANOG* promoter-*Gfp* vector (data not shown). We obtained approximately ~10 *Gfp*-positive Sc-iPC colonies from 1×10^4 cancer cells.

Quantitative RT-PCR analysis with specific primers showed that a temporal increase in the expression of four transfected genes (Tgs), *c-MYC*, *SOX2*, *OCT3/4*, and *KLF4*, was observed at day 5, although they were absent at day 0. The expression decreased to low or undetectable levels on day 30, suggesting gene silencing (Fig. 1B). In contrast, the transfected and endogenous expression levels of ES-like genes, *c-MYC*, *SOX2*, *OCT3/4*, *KLF4*, *NANOG*, and *REX1*, apparently increased at day 30, compared with those at day 0 (Fig. 1C). The Sc-iPC cells data were consistent with previous findings on non-cancerous somatic cells (iPS cells; [3]) and other cancer cells (iPC cells; [4]).

3.2. Sc-iPC cells expressed immature-related surface antigens and associated epigenetic modifications

To assess the acquisition of an immature state, Sc-iPC cells at day 30 were stained with immature-related surface antigens.

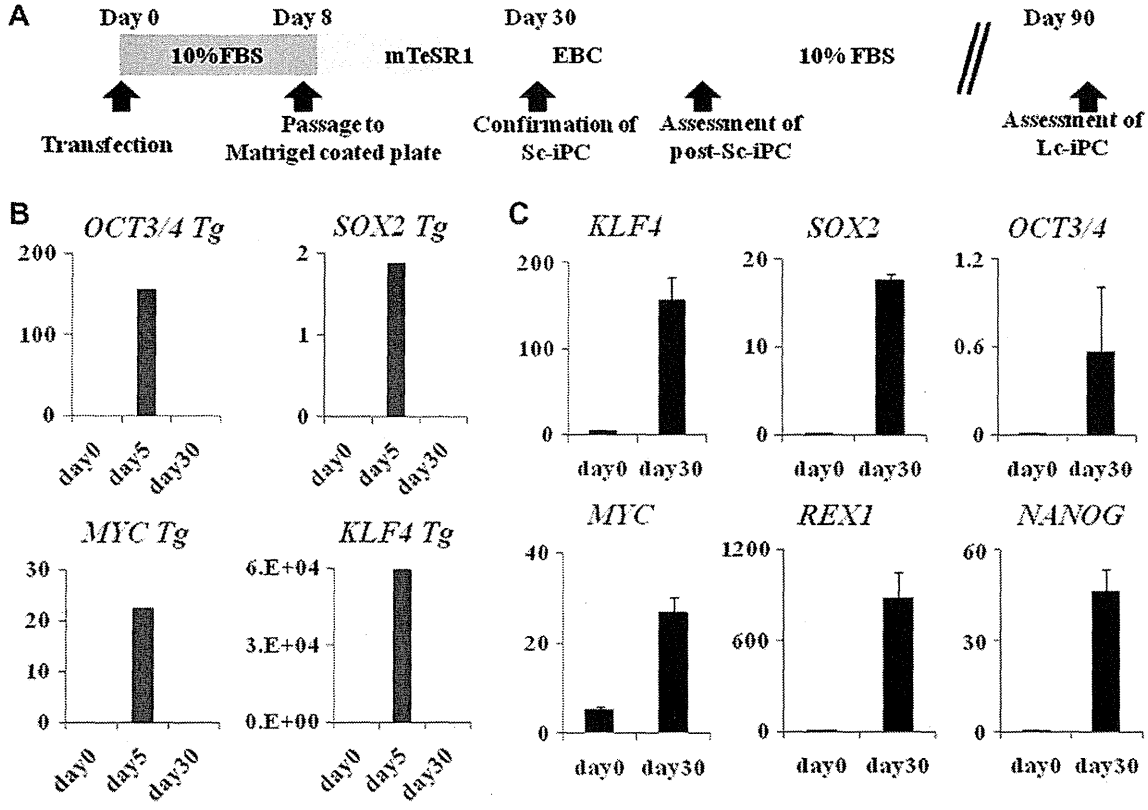

Fig. 1. Induction of ES-like genes in human GI cancer cells. Lentiviral and retroviral-mediated ES-like gene transfer induced a pluripotent state in three GI cancer cell lines to form iPC cells from three GI cancer cell lines. (A) Time course schedule of Sc-iPC, post-Sc-iPC, and Lc-iPC cells production. (B,C) Quantitative RT-PCR of Tg (B) and total mRNA (C) demonstrated temporal transgene expression after transfection and expressed undifferentiated ES-like genes *c-MYC*, *SOX2*, *OCT3/4*, *KLF4*, *NANOG*, and *REX1* in Sc-iPC cells from HuCC-T1 cells. The expression of mRNA copies was normalized against *GAPDH* mRNA expression.

Immunocytochemistry revealed that induced cells were positively stained with tumor-related antigens (Tra)-1-60, Tra-1-81, Tra-2-49, and stage-specific embryonic antigen (Ssea)-4 (Fig. 2A), indicating the maintenance of an immature state in Sc-iPC cells. Similar data were obtained for all three cell lines, and a representative result from HuCC-T1 and PLC cells are shown.

Epigenetic modifications were confirmed by assessing histone methylation. Chromatin immunoprecipitation using the trimethyl histone H3 protein at lysine 4 (H3K4) antibody indicated that H3K4 of *NANOG* and *OCT3/4* promoters were trimethylated in Sc-iPC cells, but not in parent nor post-Sc-iPC cells; post-Sc-iPC cells were prepared from Sc-iPC cells by culturing cells in embryonic body culture conditions (EBC) for 1 week and then in primary culture medium for another 1 week (Fig. 2B). Trimethylation of the *SOX2* promoter was detected in Sc-iPC cells and to a lesser extent in parental cells. The results indicated that the promoters of ES-like genes were activated in Sc-iPC cells.

3.3. Sc-iPC cells showed differentiation in vitro

To assess their ability to differentiate, we placed Sc-iPC cells in differentiation culture medium with an osteogenic or adipogenic supplement for 2 weeks (Fig. 2C and E). The data indicated that Sc-iPC cells were susceptible to differentiation, which was studied by positive staining for Osteocalcin (specific for osteocytes) or Fabp4 (specific for adipose cells), but not for parental cells (Fig. 2D and F; data not shown). Quantitative RT-PCR analysis with specific primers showed that post-Sc-iPC cells from HuCC-T1 were expressing paired box 6 (*PAX6*, representing ectoderm), microtubule-associated protein 2 (*MAP2*, representing ectoderm) and E-cadherin (*CDH1*, representing endoderm). Taken together, it is suggested that Sc-iPC cells have ability to express differentiation markers into three germ layers.

3.4. Sc-iPC cells were sensitized to differentiation-inducing reagents

The proliferation of Sc-iPC (Supplementary Fig. S2A) after 48 h incubation was not significantly different from that of parental HuCC-T1 cells. In contrast, treatment with differentiation inducers of RA or VD3 for 48 h resulted in a significant decrease in the invasiveness ratio of post-Sc-iPC cells compared to HuCC-T1 parental cells (Supplementary Fig. S2B and C). RA is commonly used for the treatment of acute promyelocytic leukemia, which involves differentiation of immature leukemic promyelocytes into mature granulocytes [6]. It has been suggested that RA or VD3 treatment is effective for inducing differentiation of post-Sc-iPC cells.

3.5. Cultured Lc-iPC cells showed increased proliferation and 5-FU resistance

In proliferation assay, Lc-iPC cells from HuCC-T1 proliferated in a high magnitude, compared with parental cells significantly (Fig. 3A). To compare the sensitivity of Lc-iPC cells to anti-cancer drugs with that of parental cells, we performed the MTT assay for 5-FU. The IC_{50} value of Lc-iPC cells from HuCC-T1 cells was significantly higher than that of parental cells (Fig. 3B), indicating that a long-term culture may elicit malignant transformation of iPC cells compared to clones immediately after inducing reprogramming [4].

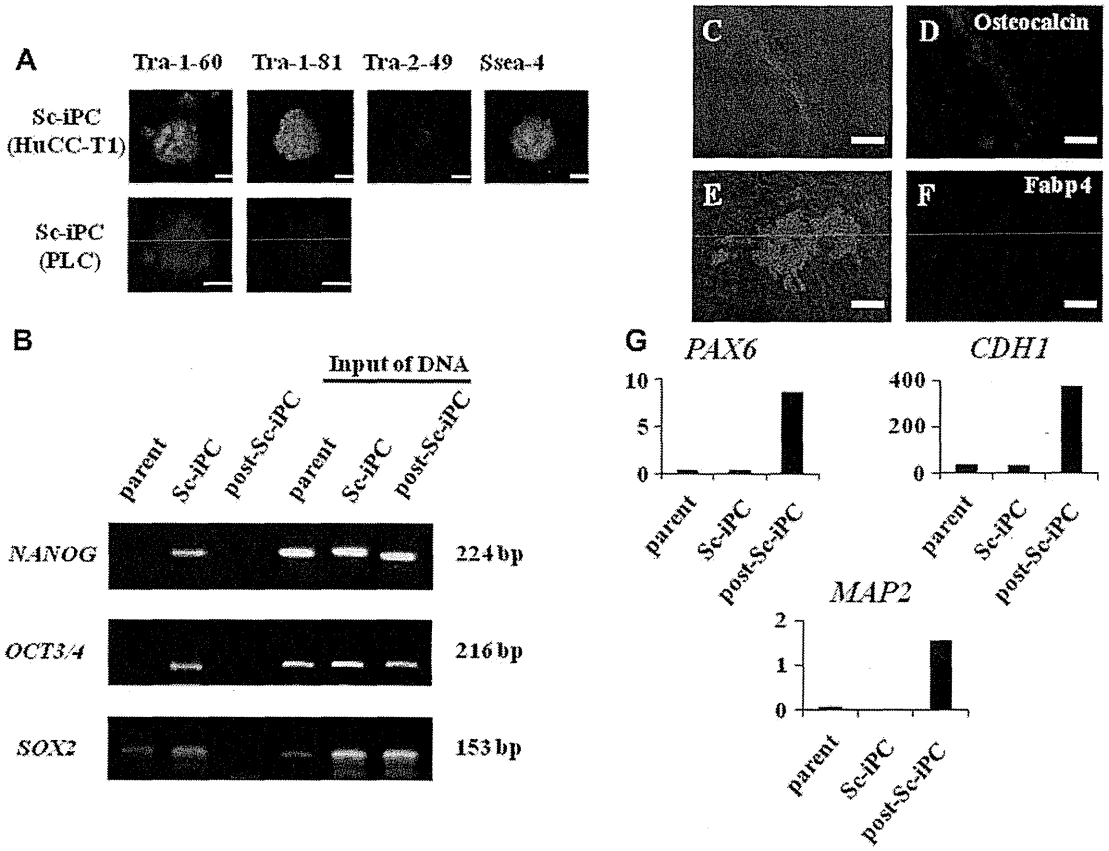

Fig. 2. An immature state and multi-differentiation potential of Sc-iPC cells. (A) Immature-related surface antigens in Sc-iPC cells from HuCC-T1 and PLC were analyzed; Tra-1-60, Tra-1-80, Tra-2-49, and Ssea-4. Bar, 200 μm; Original magnification, 200×. (B) Histone modification status in parental, Sc-iPC, and post-Sc-iPC cells from HuCC-T1 was analyzed using chromatin immunoprecipitation with the trimethyl-K4 H3 antibody. H3 lysine 4 was methylated in the promoter regions for *NANOG* and *OCT3/4* in Sc-iPC cells, but not in parental and post-Sc-iPC cells. Respective sheared chromatin samples were used as control for semi-quantitative PCR. Lineage-directed differentiation of Sc-iPC cells to osteocytes or adipocytes demonstrated that osteocyte-differentiated Sc-iPC cells (C) were positive for Osteocalcin (D) and adipocyte-differentiated Sc-iPC cells (E) were positive for Fabp4 (F). Bar, 200 μm; Original magnification, 100×. (G) *PAX6*, *CDH1*, and *MAP2* expressions were evaluated by quantitative RT-PCR in parental HuCC-T1, Sc-iPC, and post-Sc-iPC cells. The expression of mRNA copies was normalized against *GAPDH* mRNA expression.

3.6. Lc-iPC cells formed c-Myc-positive tumors in immunodeficient mice

Since the preceding proliferation assay indicated high activity, we inoculated HuCC-T1-derived Lc-iPC cells into NOD-scid mice to assess the *in vivo* tumorigenicity. Tumors were formed 4 weeks after inoculation (Fig. 3C and D). Interestingly, 8 weeks after injection the size of these tumors was significantly larger in Lc-iPC cells as compared to that in parental cells (Fig. 3E). The H-E staining indicated that tumors of Lc-iPC cells showed no apparent teratomas, but indicated the presence of a proliferating phenotype as compared to those of parental cells (Fig. 3F and G). Immunohistochemical staining with anti-c-Myc antibody indicated that Lc-iPC-formed tumors were positive for c-Myc, compared to parental cell-derived tumors (Fig. 3H and I), suggesting that c-Myc activation may play a role, at least partially, in the development of a malignant Lc-iPC cell phenotype.

3.7. Lc-iPC cells expressed the activated endogenous c-MYC gene but not other ES-like transcriptional factors

To elucidate the mechanism of activated *c-MYC* expression in Ls-iPC cell-derived tumor in NOD-scid mice, the expressions of endogenous and transgenic ES-like transcriptional factors were investigated in Lc-iPC cells from HuCC-T1. As shown in Fig. 4A, the expression of the ES-like transcriptional factor mRNAs including *SOX2, OCT3/4, KLF4, and NANOG* was decreased drastically, whereas total amount of *c-MYC* expression was detectable in an appreciable level. The origin of *c-MYC* was found to be endogenous, since transgenic *c-MYC* expression was undetected (Fig. 4B), indicating endogenous *c-MYC* activation of Lc-iPC cells increased tumorigenisity in NOD-scid mice.

3.8. Lc-iPC cells lost the expression of immature-related surface antigens and associated epigenetic modifications

To elucidate the immature status of Lc-iPC cells from HuCC-T1, we investigated immature-related surface antigens and histone modification status. Lc-iPC cells from HuCC-T1 lost their expression of immature-related surface antigens including Tra-1-60, Tra-1-81, Tra-2-49, and Ssea-4 (Supplementary Fig. S3); *NANOG, OCT3/4,* and *SOX2* promoters of Lc-iPC cells were slightly trimethylated, indicating that these three ES-like genes were inactivated (Fig. 4C), and suggesting that *c-MYC* is prone to activation in the Lc-iPC cells.

4. Discussion

GI cancer is a major cause of death in several developed countries, including Japan. After therapeutic interventions, such

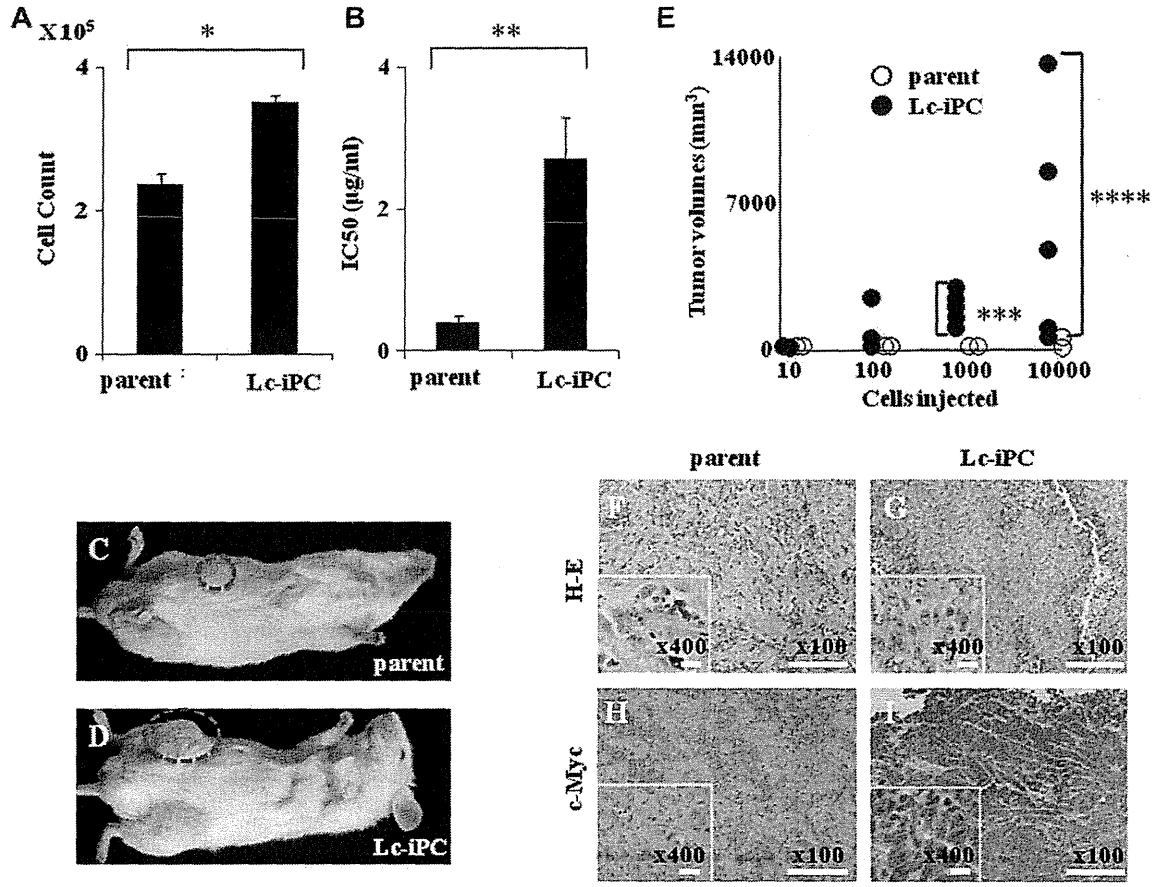

Fig. 3. MTT assay, proliferation *in vitro*, tumor formation *in vivo*, and c-Myc immunohistochemistry by induced Lc-iPC cells from HuCC-T1. Proliferation assay showed an increased proliferation (A; $n = 5$, $^{*}p = 0.012$) and MTT assay showed an increased IC_{50} for 5-FU (B; $n = 7$, $^{**}p = 0.001$) in Lc-iPC cells from HuCC-T1 as compared with parental cells. Lc-iPC and parental cells from HuCC-T1 were subcutaneously transplanted into three parts of NOD-scid mice. Four weeks after injection (C and D), tumors were palpable subcutaneously. Tumors were dissected and measured 8 weeks after injection. Tumors from Lc-iPC cells were larger than those from parental cells when 1000 and 10,000 cells were injected ($n = 6$, $^{***}p = 0.005$, $^{****}p = 0.005$, respectively). H–E staining of dissected tumor, (F) parental cells from HuCC-T1; (G) Lc-iPC cells from HuCC-T1. Tumors from Lc-iPC cells were less differentiated than parental cells. c-Myc immunohistochemistry showed that tumors of Lc-iPC cells from HuCC-T1 (I) expressed c-Myc protein more than those from parental cells (H). Bar, 100 μm; Original magnification, 100×, 400×.

as surgery and conventional chemoradiation therapy, tumor reduction and remission occur in more than half of the cases, although tumors can relapse and spread to other organs, i.e., metastasis. To overcome resistance to therapy, we recently showed that GI cancer reprogramming can sensitize cancer cells to differentiation and chemotherapeutic agents [4], indicating that further investigation is required on reprogramming of cancer cells to discover novel therapeutic approaches.

Several studies have reported reprogramming of cancer cells, including skin cancer or melanoma cells, using vectors harboring micro RNA-302 [7], *OCT3/4*, *c-MYC*, and *KLF4* [8], by nuclear transplantation [9]; but also GI cancer by introducing ES-like genes, which have been mentioned as iPS genes [4]. Introducing defined factors could be the advancement for science and technology as compared with reprogramming by nuclear transplantation, which might be necessary for determining safety issues. iPS cells, similar to ES cells, have the potential to form teratomas following inoculation in immunodeficient mice, presumably through the involvement of retroviral integration, retaining immature clones, and oncogenic *c-MYC* activation, which is consistent with the findings of the present study.

However, the involvement of *c-MYC* should be further investigated. A previous report indicated that tumors formed in iPS cell-derived chimeric mice could be attributed to the reactivation of the *c-MYC* retroviral transgene [10], whereas another report stated that the propensity for teratoma formation from a secondary neurosphere, derived from mice iPS cells, may depend on the tissue of origin but not on *c-MYC* transgene reactivation [11]. In our study, induced Lc-iPC cells showed increased proliferation and chemoresistance to 5-FU and stained strongly positive for c-Myc, which may be relevant to endogenous c-Myc activation in tumors, as detected by quantitative RT-PCR (Fig. 4A and B).

Nevertheless, we must consider other factors involved in iPC cells induction, such as genomic abnormalities, which are the usual characteristics of cancer cells. A possibility is that $TP53^{R175H}$ and $KRAS^{G12D}$ genomic mutations of HuCC-T1 may be relevant to the present observation [13] (data not shown). $KRAS^{G12D}$, a common mutation in solid cancers, is an active form of the *KRAS* gene. Mice expressing oncogenic $Kras^{G12D}$ and mutant *Tp53* accelerated the onset of cancer [12]. Taken together, data suggest that HuCC-T1 reprogramming may affect the pathways of these two mutated proteins.

Based on our results, we are confident of developing more effective differentiation therapies to conquer cancer if we find more appropriate differentiation pathways; however, further analysis of Sc-iPC and Lc-iPC cell properties is needed. Our data suggest that this new reprogramming technology will be a key to conquer bile duct carcinoma through its high magnitude of effect on sensitiza-

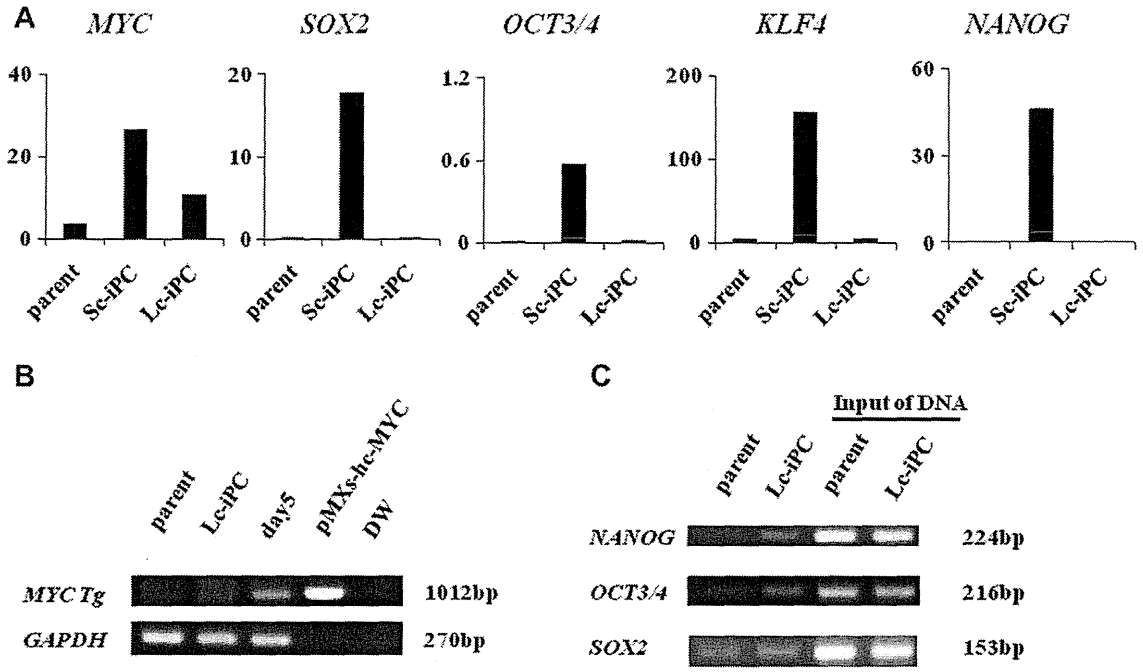

Fig. 4. Immature state of induced Lc-iPC cells from HuCC-T1. (A) Quantitative RT-PCR of total mRNAs of ES-like genes demonstrated genes expression, including *c-MYC*, *SOX2*, *OCT3/4*, *KLF4*, and *NANOG*, of Lc-iPC cells from HuCC-T1, decreased drastically compared to that of Sc-iPC cells except *c-MYC*. The expression of mRNA copies was normalized against *GAPDH* mRNA expression. (B) The RT-PCR of Lc-iPC from HuCC-T1 did not detect transgene (*Tg*) *c-MYC*. Day5, HuCC-T1 cells five days after transfection (*c-MYC*, *SOX2*, *OCT3/4*, and *KLF4*); pMXs-hc-MYC, positive control reaction of vector; DW, negative control with water. (C) Histone modification status in parental and Lc-iPC cells from HuCC-T1 was analyzed using chromatin immunoprecipitation with anti-trimethyl-K4 H3 antibody. The methylation signal at H3 lysine 4 was detected slightly in *NANOG*, *OCT3/4* and *SOX2* promoters in Lc-iPC cells, and *SOX2* in parental cells.

tion to a series of reprogramming-mediated, anti-cancer therapies, and that a predictive method will be necessary for evaluating the improper reprogramming-associated aggressive phenotype of iPC cells. In future, a day will come when cancer will be cured more effectively by newly discovered pharmacogenomic medicine based on reprogramming technology.

5. Conclusion

Although defined factor-induced reprogramming of gastrointestinal cancer cells is a promising approach for the treatment of cancer, we noted that Lc-iPC cells may be prone to genomic instability presumably due to genetic and epigenetic alterations including endogenous *c-MYC* activation, which is characteristic of cancer cells and is associated with reprogramming technology. To exclude therapy-resistant clones in GI cancer, it is necessary to develop a predictive method for evaluating improper reprogramming-associated aggressive phenotype of reprogrammed cells.

Acknowledgments

We thank Dr. Gregory J. Gores, Mayo Clinic College of Medicine, Rochester, MN, for providing cholangiocellular carcinoma HuCC-T1 cells and Kimie Kitagawa for excellent technical assistance. This work was supported in part by a Grant-in-Aid for Scientific Research on Priority Areas (20012039), a Grant-in-Aid for Scientific Research (S, 21229015; C, 20590313), and a Grant-in-Aid for Young Scientists (B, 21791287) from the Ministry of Education, Culture, Sports, Science, and Technology, Japan; the Kobayashi Foundation for Cancer Research and the Uehara Memorial Foundation, Japan.

Appendix A. Supplementary data

Supplementary data associated with this article can be found, in the online version, at doi:10.1016/j.bbrc.2010.03.176.

References

[1] A.P. Feinberg, R. Ohlsson, S. Henikoff, The epigenetic progenitor origin of human cancer, Nat. Rev. Genet. 7 (2006) 21–33.
[2] T. Reya, S.J. Morrison, M.F. Clarke, et al., Stem cells, cancer, and cancer stem cells, Nature 414 (2001) 105–111.
[3] K. Takahashi, K. Tanabe, M. Ohnuki, et al., Induction of pluripotent stem cells from adult human fibroblasts by defined factors, Cell 131 (2007) 861–872.
[4] N. Miyoshi, H. Ishii, K. Nagai, et al., Defined factors induce reprogramming of gastrointestinal cancer cells, PNAS 107 (2010) 40–45.
[5] S. Yamanaka, Elite and stochastic models for induced pluripotent stem cell generation, Nature 460 (2009) 49–52.
[6] A. Kakizuka, W.H. Miller Jr., K. Umesono, et al., Chromosomal translocation *t*(15;17) in human acute promyelocytic leukemia fuses RAR alpha with a novel putative transcription factor, PML, Cell 66 (1991) 663–674.
[7] S.L. Lin, D.C. Chang, S. Chang-Lin, et al., Mir-302 reprograms human skin cancer cells into a pluripotent ES-cell-like state, RNA 14 (2008) 2115–2124.
[8] J. Utikal, N. Maherali, W. Kulalert, et al., Sox2 is dispensable for the reprogramming of melanocytes and melanoma cells into induced pluripotent stem cells, J. Cell Sci. 122 (2009) 3502–3510.
[9] K. Hochedlinger, R. Blelloch, C. Brennan, et al., Reprogramming of a melanoma genome by nuclear transplantation, Genes Dev. 18 (2004) 1875–1885.
[10] K. Okita, T. Ichisaka, S. Yamanaka, Generation of germline-competent induced pluripotent stem cells, Nature 448 (2007) 313–317.
[11] K. Miura, Y. Okada, T. Aoi, et al., Variation in the safety of induced pluripotent stem cell lines, Nat. Biotechnol. 27 (2009) 743–745.
[12] L. Johnson, K. Mercer, D. Greenbaum, et al., Somatic activation of the K-ras oncogene causes early onset lung cancer in mice, Nature 410 (2001) 1111–1116.

Web reference

[13] Available from: http://www.sanger.ac.uk, last accessed date, July 15, 2009.

THE JOURNAL OF BIOLOGICAL CHEMISTRY VOL. 285, NO. 46, pp. 35274–35283, November 12, 2010

Characterization of Leukocyte Mono-immunoglobulin-like Receptor 7 (LMIR7)/CLM-3 as an Activating Receptor

*ITS SIMILARITIES TO AND DIFFERENCES FROM LMIR4/CLM-5**

Received for publication, April 26, 2010, and in revised form, July 30, 2010 Published, JBC Papers in Press, September 3, 2010, DOI 10.1074/jbc.M110.137166

Yutaka Enomoto[‡], Yoshinori Yamanishi[‡], Kumi Izawa[‡], Ayako Kaitani[‡], Mariko Takahashi[‡], Akie Maehara[‡], Toshihiko Oki[‡§], Reiko Takamatsu[¶], Masunori Kajikawa[¶], Toshiyuki Takai[‖], Toshio Kitamura[‡§1], and Jiro Kitaura[‡2]

From the [‡]Division of Cellular Therapy, Advanced Clinical Research Center, Institute of Medical Science, and the [§]Division of Stem Cell Signaling, Center for Stem Cell Therapy, Institute of Medical Science, The University of Tokyo, 4-6-1 Shirokanedai, Minato-ku, Tokyo 108-8639, Japan, [¶]ACTGen Inc., 15-502 Akaho, Komagane-shi, Nagano-ken 399-4117, Japan, and the [‖]Department of Experimental Immunology, Institute of Development, Aging, and Cancer, Tohoku University, 4-1 Seiryo, Sendai 980-8575, Japan

Here we characterize leukocyte mono-Ig-like receptor 7 (LMIR7)/CLM-3 and compare it with an activating receptor, LMIR4/CLM-5, that is a counterpart of an inhibitory receptor LMIR3/CLM-1. LMIR7 shares high homology with LMIR4 in the amino acid sequences of its Ig-like and transmembrane domains. Flow cytometric analysis demonstrated that LMIR4 was predominantly expressed in neutrophils, whereas LMIR7 was highly expressed in mast cells and monocytes/macrophages. Importantly, LMIR7 engagement induced cytokine production in bone marrow-derived mast cells (BMMCs). Although FcRγ deficiency did not affect surface expression levels of LMIR7, it abolished LMIR7-mediated activation of BMMCs. Consistently we found significant interaction of LMIR7-FcRγ, albeit with lower affinity compared with that of LMIR4-FcRγ. Our results showed that LMIR7 transmits an activating signal through interaction with FcRγ. In addition, like LMIR4, LMIR7 synergizes with TLR4 in signaling. Analysis of several chimera receptors composed of LMIR4 and LMIR7 revealed these findings: 1) the transmembrane of LMIR7 with no charged residues maintained its surface expression at high levels in the absence of FcRγ; 2) the extracellular juxtamembrane region of LMIR7 had a negative effect on its surface expression levels; and 3) the strong interaction of LMIR4 with FcRγ depended on the extracellular juxtamembrane region as well as the transmembrane domain of LMIR4. Thus, LMIR7 shares similarities with LMIR4, although they are differentially regulated in their distribution, expression, and function.

A new family of paired immunoreceptors has been recently identified and named leukocyte mono-Ig-like receptor (LMIR)[3]/CMRF-35-like molecules (CLM)/myeloid-associated Ig-like receptor (MAIR)/dendritic cell-derived Ig-like receptor (DIgR)/immune receptor expressed by myeloid cell (IREM)/CD300 (1–15). In mice, there exist at least eight members of the LMIR family (1–9). We and others have previously characterized LMIR1–5 (1–8). An inhibitory receptor, LMIR3/CLM-1, pairs with an activating receptor, LMIR4/CLM-5 or LMIR5/CLM-7. LMIR3 is 91 and 53% identical with LMIR4 and LMIR5, respectively, in the amino acid sequence of the Ig-like domain. In addition, LMIR4 and LMIR5 transmits an activating signal through interaction with FcRγ and DAP12, respectively (2, 3). Consistently, LMIR5 has a positively charged residue (lysine) in the transmembrane domain, which is characteristic of activating receptors interacting with adaptors containing ITAM (3). However, LMIR4 does not have a positively charged residue in the transmembrane domain; instead, it has a negatively charged residue (glutamic acid) (2, 8). Interestingly, the inhibitory receptor LMIR3 also has the potential to transmit an activating signal through interaction with FcRγ in mast cells, despite having no charged residue in the transmembrane domain (4).

FcRγ is an ITAM-bearing signal transduction subunit expressed in a variety of hematopoietic cells (15–19). It is an essential component of the high affinity receptor for IgE (FcεRI) (17), the high affinity IgG receptor (FcγRI) (18), the low affinity IgG receptor (FcγRIII) (19), and the IgA receptor (FcαRI) (20, 21). In addition, FcRγ interacts with various activating receptors such as paired Ig-like receptor A (PIR-A) (22) or platelet collagen receptor glycoprotein VI (23). Although the Arg/Asp charge interaction between transmembrane domains is well characterized, recent studies have also implicated a transmembrane leucine zipper-like interaction between activating receptors and FcRγ (24, 25). However, the relevant molecular mechanism remains incompletely understood.

In the present study, we have characterized LMIR7/CLM-3, which had not been fully analyzed. Structurally, LMIR7 is similar to LMIR4 in its Ig-like and transmembrane domains. The generation of an antibody specifically reacting with LMIR7 enabled us to delineate the differential expression profiles of

* This work was supported by the Ministry of Education, Science, Technology, Sports, and Culture and the Ministry of Health and Welfare, Japan.

[1] To whom correspondence may be addressed: Division of Cellular Therapy, Advanced Clinical Research Center, Inst. of Medical Science, University of Tokyo, 4-6-1 Shirokanedai, Minato-ku, Tokyo 108-8639, Japan. Tel.: 81-3-5449-5759; Fax: 81-3-5449-5428; E-mail: kitamura@ims.u-tokyo.ac.jp.

[2] To whom correspondence may be addressed: Division of Cellular Therapy, Advanced Clinical Research Center, Inst. of Medical Science, University of Tokyo, 4-6-1 Shirokanedai, Minato-ku, Tokyo 108-8639, Japan. Tel.: 81-3-5449-5759; Fax: 81-3-5449-5428; E-mail: kitaura-tky@umin.ac.jp.

[3] The abbreviations used are: LMIR, leukocyte mono-immunoglobulin-like receptor; CLM, CMRF-35-like molecule; BM, bone marrow; PB, peripheral blood; FLMC, fetal liver-derived mast cell; BMMC, bone marrow-derived mast cell; BMMΦ, bone marrow-derived macrophage; BMmDC, bone marrow-derived myeloid dendritic cell; BMpDC, bone marrow-derived plasmacytoid dendritic cell; SCF, stem cell factor; ITAM, immunoreceptor tyrosine-based activation motif; Ab, antibody; PE, phycoerythrin.

LMIR7 and LMIR4. Importantly, LMIR7 engagement led to the activation of bone marrow-derived mast cells (BMMCs) through interaction with FcRγ, validating an activating function of LMIR7 similar to that of LMIR4. Notably, analysis of chimera receptors composed of LMIR4 and LMIR7 revealed that a short extracellular juxtamembrane region of LMIR4 played an important role in its strong interaction with FcRγ. This finding will likely lead us to uncover novel regulatory mechanisms in the interaction of a diverse array of activating receptors with FcRγ.

EXPERIMENTAL PROCEDURES

Antibodies and Other Reagents—Rat anti-LMIR7 IgG_1 monoclonal Ab (mAb) was generated by ACTGen Inc. Anti-FLAG mAb (M2), fluorescein isothiocyanate (FITC)-conjugated anti-FLAG mAb (M2), rabbit anti-FLAG Ab, mouse IgG_1 mAb (MOPC21), and mouse anti-dinitrophenyl (DNP) IgE mAb (SPE-7) were purchased from Sigma-Aldrich. Mouse anti-Myc mAb (9E10) was from Roche Diagnostics. PE- or FITC-conjugated anti-c-Kit, FcεRIα, CD3, B220, NK1.1, F4/80, CD11b, CD11c, or Gr-1 mAbs, Rat IgG_1 mAb, and PE-conjugated streptavidin were from eBioscience. PE-conjugated anti-mouse IgG goat $F(ab')_2$ Ab was from Beckman Coulter. Anti-ERK Ab was from Santa Cruz Biotechnology. Rabbit anti-FcεRI-γ subunit Ab was purchased from Upstate Biotechnology. All of the phospho-specific Abs was purchased from Cell Signaling Technology. Cytokines were obtained from R&D Systems. All other reagents were from Sigma-Aldrich unless stated otherwise.

Cell Culture and Isolation—Murine hematopoietic cell lines and 293T cells were cultured as described (2, 3). C57BL/6 mice (Charles River Laboratories Japan Inc.) were used at 8–10 weeks of age for isolation of tissues and cells such as BM cells, peripheral blood (PB) cells, peritoneal cells, splenocytes, and thymocytes as described (2, 3). All procedures were approved by an institutional review committee. To generate BMMC or fetal liver-derived mast cells (FLMC) with 90% purity (c-Kit^+/$FcεRI^+$ by flow cytometry), BMMCs or FLMCs were cultured in the presence of 10 ng/ml IL-3 alone or with 20 ng/ml stem cell factor (SCF) as described (2–4, 26–29). To generate BM-derived macrophages (BMMΦ), BM-derived myeloid dendritic cells (BMmDC), and BM-derived plasmacytoid dendritic cells (BMpDC), BM cells were cultured in the presence of 10 ng/ml M-CSF, 20 ng/ml GM-CSF, and 50 ng/ml Flt3-ligand, respectively, as described (2–4). BMmDC or BMpDC were sorted by using FITC-conjugated anti-CD11c Ab. BM granulocytes were prepared as described (3). The following mutant mice were used: *FcRγ*$^{-/-}$ (16), *DAP10*$^{-/-}$ (30), and *DAP12*$^{-/-}$ (31).

Gene Expression Analysis—Expression of LMIR7 was analyzed by reverse transcriptase-polymerase chain reaction (RT-PCR) as described (2, 3). Total RNAs were extracted from each cell line and BM-derived cells with TRIzol reagents (Invitrogen), treated with deoxyribonuclease I (Invitrogen), and reverse-transcribed by using High Capacity cDNA Reverse Transcription Kits (Applied Biosystems). A fragment of LMIR7 was amplified with primers 5′-acacccacaacaccaaccac-3′ and 5′-ctgggaagtgtttctctccg-3′. For normalization, a fragment of β-actin was amplified with 5′-catcactattggcaacgagc-3′ and 5′-acgcagctcagtaacagtcc-3′. Relative expression levels of LMIR7 among samples were measured by real-time RT-PCR as described (3). cDNA was amplified using a LightCycler FastStart DNA Master SYBR Green I Kit (Roche Diagnostics) under the following conditions: one cycle of 95 °C for 10 s, 40 cycles of 95 °C for 5 s, and 60 °C for 25 s. All samples were independently analyzed three times. The following primers were used: 5′-acacccacaacaccaaccac-3′ and 5′-accacaaagaccatcagcaaga-3′ for LMIR7; and 5′-atgtgtccgtcgtggatctga-3′ and 5′-ttgaagtcgcaggagacaacct-3′ for GAPDH. Relative gene expression levels were calculated using standard curves generated by serial dilution of cDNA and normalized by a GAPDH expression level. Product quality was checked by melting curve analysis via LightCycler software (Roche Diagnostics).

Plasmid Constructs—We searched the GenBank™/European Molecular Biology Laboratory (EMBL)/DNA Data Bank of Japan (DDBJ) database by using the amino acid sequence of the Ig-like domain of mLMIR1. On the basis of the sequence data, the cDNA of mouse LMIR7 was isolated by PCR with the primers 5′-caccaaggacaggagaggag-3′ and 5′-agggagagggagagggaga-3′ from a cDNA library of BMMCs derived from C57BL/6 mice and its sequence was confirmed (LMIR7/CLM-3: GenBank™ accession number AY457049) (1–3). A cDNA fragment of LMIR7 lacking the signal sequence was tagged with a FLAG or Myc epitope at the N terminus. A SLAM (signaling lymphocyte-activating molecule) signal sequence (32) (a gift from Hisashi Arase, Osaka University, Osaka, Japan), FLAG- or Myc-LMIR7, was subcloned into a pMXs-IRES-puro^r (pMXs-IP) (33) retroviral vector to generate pMXs-FLAG- or Myc-LMIR7-IP. pMXs-FLAG- or Myc-LMIR4-IP and pMXs-FcRγ-IRES-blasticidin (pMXs-FcRγ-IB) were generated as described (2–4). To generate LMIR7 mutants (LMIR7-M1, -M2, and -M3) or LMIR4 mutants (LMIR4-M1 and -M2), two-step PCR mutagenesis (2–4) was performed by using pMXs-FLAG-LMIR7-IP or pMXs-FLAG-LMIR4-IP, respectively, as a template. LMIR7-M1 is the LMIR7(S189Y,V197E,V198L) mutant; LMIR7-M2 is the LMIR7(^{177}NSLFIW^{182}SRPHTR) mutant where six amino acid residues (NSLFIW) of LMIR7 were replaced with six amino acid residues (SRPHTR) of LMIR4 in the extracellular juxtamembrane region; LMIR7-M3 is the LMIR7(^{177}NSLFIW^{182}SRPHTR,S189Y,V197E,V198L) mutant; LMIR4-M1 is the LMIR4(Y177S,E185V,L186V) mutant; and LMIR4-M2 is the LMIR4(^{165}SRPHTR^{170}NSLFIW) mutant where six amino acid residues (SRPHTR) of LMIR4 were replaced with six amino acid residues (NSLFIW) of LMIR7 in the extracellular juxtamembrane region. All constructs were verified by DNA sequencing.

Transfection and Infection—Retroviral transfection was as described (1–4, 33, 34). Briefly, retroviruses were generated by transient transfection of PLAT-E packaging cells (34) with FuGENE 6 (Roche Diagnostics). Cells were infected with retroviruses in the presence of 10 μg/ml Polybrene. Selection with puromycin or blasticidin was started 48 h after infection.

Biochemistry—BMMCs expressing FLAG-tagged LMIR7 or mock were stimulated by 10 μg/ml anti-FLAG mAb or mouse IgG_1 mAb as control, 50 ng/ml SCF, or 10 μg/ml SPE-7 IgE for the indicated time as described (2–4, 28). To detect phosphorylation of several proteins, stimulated cells were lysed with Nonidet P-40 lysis buffer containing protease and phosphatase

inhibitor mixture (Sigma-Aldrich). To detect the interaction of LMIR7 and FcRγ, 293T cells were co-transfected with two constructs of interest. Cells were lysed with digitonin lysis buffer containing protease and phosphatase inhibitor mixture. Immunoprecipitation and Western blotting were done as described (1–4).

Flow Cytometry—Flow cytometric analysis of the stained cells was performed with a FACSCalibur (BD Biosciences) equipped with CellQuest software and Flowjo software (Tree Star) as described (2–4). Anti-LMIR7 mAb or rat IgG_1 mAb as control was biotinylated by sulfo-NHS-LC-biotin (Pierce) according to the manufacturer's instructions. Cells were incubated with 20 μg/ml biotin-anti-LMIR7 mAb or biotin-anti-rat IgG_1 mAb before incubation with PE-conjugated streptavidin. The geometric mean fluorescence intensity of Myc-tagged LMIR4, LMIR7, or its mutants was measured to evaluate its surface expression levels.

Measurement of Cytokines and Chemokines—For efficient stimulation of BMMC or FLMC, anti-biotin MACSiBead particles (Miltenyi Biotec) were used. Briefly, we prepared equal numbers of anti-biotin MACSiBead particles loaded with equal amounts of biotinylated anti-FLAG Ab, mouse IgG_1 mAb, anti-LMIR7 mAb, or rat IgG_1 mAb according to the manufacturer's instructions. Cells were stimulated by adding 2×10^6 anti-biotin MACSiBead particles to 1.5×10^5 cells in the presence or absence of 100 ng/ml lipopolysaccharide (LPS). After 24 h of stimulation, the concentrations of cytokines/chemokines in the supernatants were measured using enzyme-linked immunosorbent (ELISA) kits of IL-6, TNF-α, or MCP-1 from R&D Systems (2–4).

Statistical Analysis—Data are shown as the mean ± S.D., and statistical significance was determined by Student's *t* test with $p < 0.05$ taken as statistically significant.

RESULTS

Structure of LMIR7 in Comparison with LMIR4—We originally cloned LMIR1 using a signal sequence trap based on a retrovirus-mediated signal sequence trap (1, 35). LMIR2, -3, -4, and -5 were cloned by searching the GenBank™/EBI/DDBJ data bank using the sequence of the Ig-like domain of LMIR1 (1–3). Similarly, LMIR7 was cloned and identified from a BMMC cDNA library. LMIR7 protein from C57BL/6 mice is 245 amino acids in length. Like LMIR2, -4, and -5, LMIR7 is a type I transmembrane protein composed of an N-terminal signal peptide, an extracellular domain containing a single V-type Ig domain, a transmembrane domain, and a short cytoplasmic tail without any signaling motif. However, unlike typical activating receptors such as LMIR2 and LMIR5 (1–3), LMIR7 does not possess a positively charged residue in the transmembrane domain. An Ig-like domain of LMIR7 shares 85% identity at amino acid sequences with that of an inhibitory receptor, LMIR3/CLM-1, or an activating receptor, LMIR4/CLM-5 (Fig. 1*A*). In addition, LMIR7 differs from LMIR4 by only three amino acids in the transmembrane domain (Fig. 6*A*). The structural resemblance of LMIR7 to LMIR4 led us to analyze LMIR7 in comparison with LMIR4. First, we generated Ba/F3 cells expressing FLAG-tagged LMIR7, LMIR3, or LMIR4. Flow cytometric analysis using anti-FLAG mAb confirmed surface

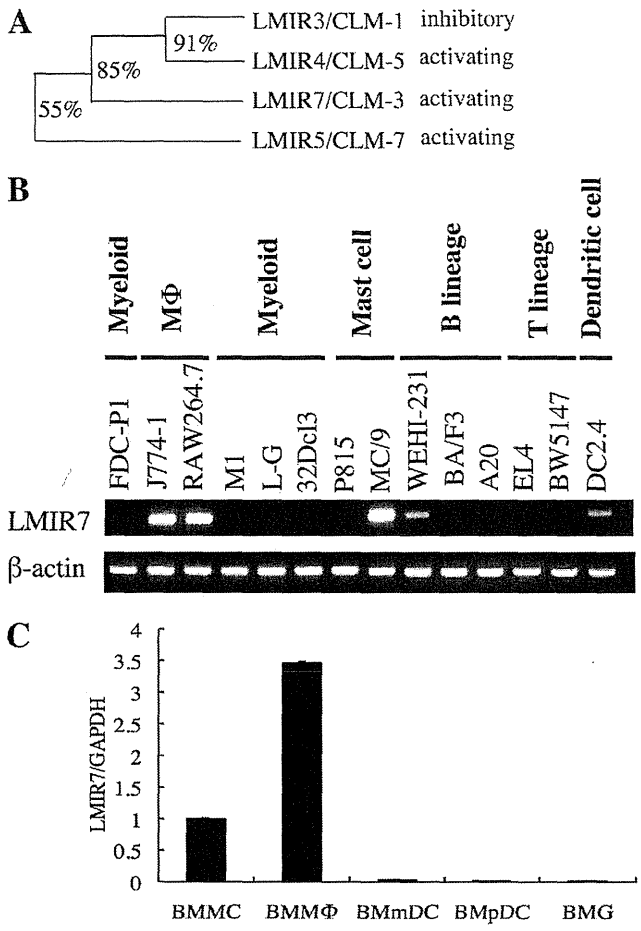

FIGURE 1. **LMIR7 expression at transcript levels in hematopoietic cells.** *A*, the phylogenetic tree of LMIR3/4/5/7 is shown based on homology with the Ig-like domain. The percentage of identity in amino acid sequences of the Ig-like domain was indicated. *B*, RT-PCR analysis on LMIR7 expression in murine hematopoietic cell lines. *C*, relative expression levels of LMIR7 among BMMC, BMMΦ, BMmDC, BMpDC, and BM granulocytes (*BMG*) were estimated by real-time PCR. The amount of expression was indicated relative to that in BMMC. Data are representative of three independent experiments.

expression of the transduced LMIR7 as well as LMIR3 and -4 (Fig. 2*A*). In addition, Western blot analysis demonstrated that similar to LMIR4, LMIR7 was detected by anti-FLAG mAb as two discrete bands (of 37 and 26 kDa) irrespective of reducing or nonreducing conditions (Fig. 2*B* and data not shown). Notably, LMIR7 were expressed more efficiently than LMIR4 at both surface expression and total protein levels (Fig. 2, *A* and *B*). Because LMIR7 protein possesses no apparent *N*-linked glycosylation sites but several *O*-glycosylation sites within its extracellular domain, we speculated that a band (37 kDa) corresponds to an *O*-glycosylated form of LMIR7 expressed on the cell surface. In accordance with this, *N*-glycosidase F treatment did not affect the mobility of LMIR7 (data not shown).

LMIR7 Is Highly Expressed in Mast Cells and Moncytes/Macrophages—To investigate the expression profile of LMIR7 in hematopoietic cells, we performed RT-PCR in a variety of hematopoietic cell lines. As a result, high expression levels of LMIR7 were observed in macrophage cell lines J774-1 and RAW264.7 and mast cell line MC/9 (Fig. 1*B*). In addition, we found detectable expression of LMIR7 in B-lineage cell lines

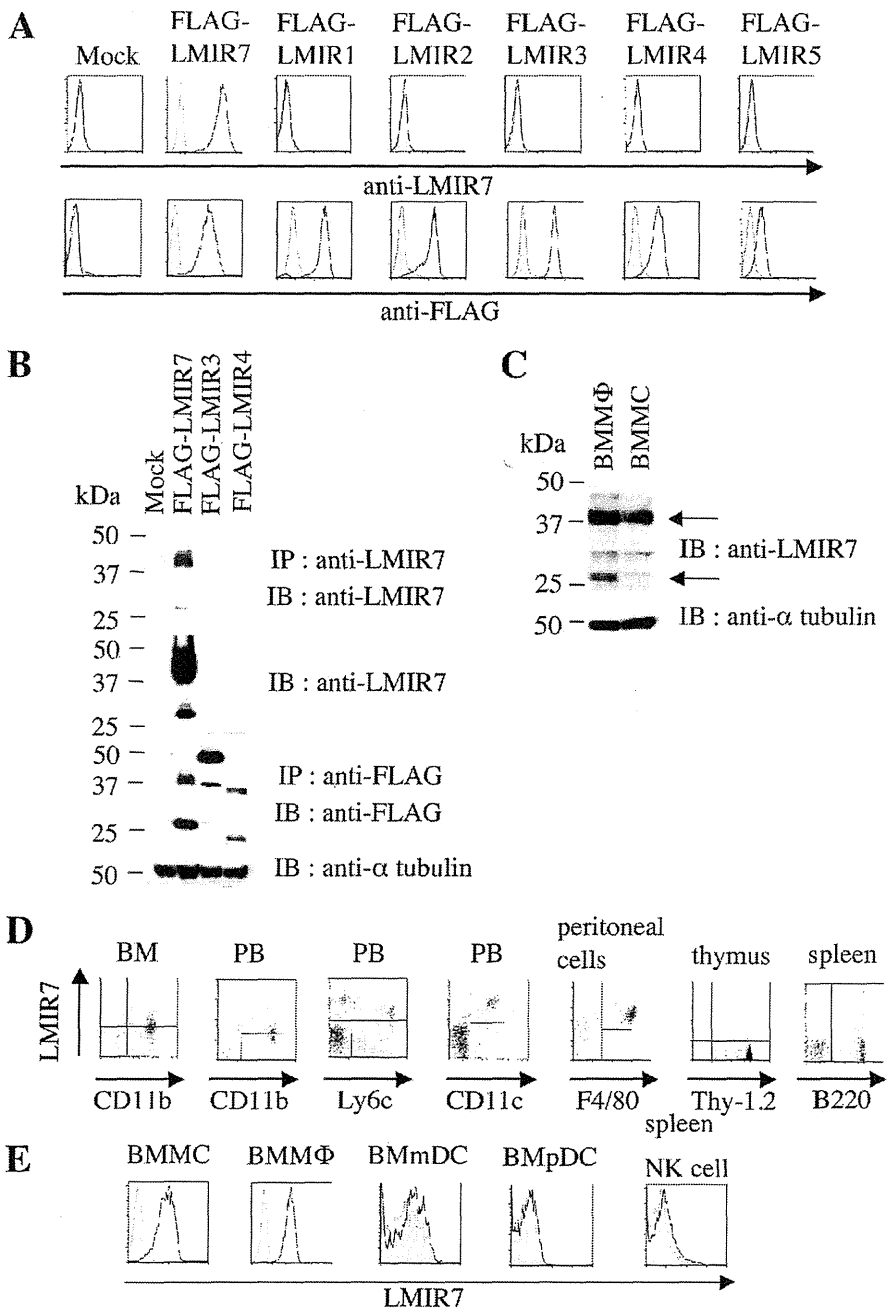

FIGURE 2. **Cell surface expression of LMIR7 in hematopoietic cells.** *A* and *B*, the sensitivity and specificity of anti-LMIR7 mAb were confirmed by flow cytometry (*A*) and Western blot (*B*). *A*, Ba/F3 cells were transduced with FLAG-tagged LMIR1, -2, -3, -4, -5, -7, or mock. The cells were stained with rat anti-LMIR7 mAb (*upper panel*) or mouse anti-FLAG mAb (*lower panel*) followed by PE-conjugated anti-rat IgG_1 Ab or anti-mouse IgG_1 Ab, respectively. *B*, lysates of Ba/F3 cells expressing FLAG-tagged LMIR3, -4, -7, or mock were immunoprecipitated with anti-LMIR7 mAb or rabbit anti-FLAG Ab and then immunoblotted with anti-LMIR7 mAb (*top panel*) or mouse anti-FLAG mAb (*third panel*), respectively. Total cell lysates were also immunoblotted with anti-LMIR7 mAb (*second panel*) or anti-α-tubulin Ab (*bottom panel*). *IB* and *IP* indicate immunoblot and immunoprecipitation, respectively. *C*, total cell lysates of BMMΦ or BMMC were immunoblotted with anti-LMIR7 mAb (*upper panel*) or anti-α-tubulin Ab (*lower panel*). *D*, analysis of LMIR7 expression in hematopoietic cells derived from C57 BL/6 mice. Single cell suspensions were prepared from BM, PB, peritoneal cavity, thymus, and spleen. Cells were stained with biotin anti-LMIR7 mAb or biotin rat IgG_1 mAb followed by PE-conjugated streptavidin and FITC-conjugated Abs as indicated. $FSC^{high}SSC^{high}$ populations in granulocytes or macrophages, $FSC^{low/int}SSC^{low/int}$ populations in lymphocytes cells, NK cells, or DC, or $FSC^{int}SSC^{int}$ populations in monocytes were gated and analyzed for LMIR7 expression. *E*, BMMC, BMMΦ, BMmDC, BMpDC, or $NK1.1^+$ spleen cells were stained with biotin anti-LMIR7 mAb or biotin rat IgG_1 mAb followed by PE-conjugated streptavidin. The result of control or LMIR7 staining is shown as a *filled* or *bold line histogram*, respectively. $NK1.1^+$ cells were sorted from spleen cells by using FITC-conjugated anti-NK1.1 Ab.

WEHI-231 and A20 and in a DC line, DC2.4, but not in other myeloid cell lines or T-lineage cell lines (Fig. 1*B*). On the other hand, real-time PCR analysis using BM-derived cells showed that expression levels of LMIR7 transcripts were specifically higher in BMMC and BMMΦ compared with BMmDC, BMpDC, or BM granulocytes (Fig. 1*C*, *BMG*). To examine the expression profiles of LMIR7 at protein levels, next we generated anti-LMIR7 mAb. As depicted in Fig. 2*A*, anti-LMIR7 mAb efficiently detected LMIR7 expressed on the surface of Ba/F3 cells transduced with FLAG-tagged LMIR7. This Ab did not detect any LMIR1, LMIR2, LMIR3, LMIR4, or LMIR5 transduced into Ba/F3 cells (Fig. 2*A*). These results verified the sensitivity and specificity of anti-LMIR7 mAb. Moreover, similar to anti-FLAG mAb, anti-LMIR7 mAb detected only FLAG-tagged LMIR7 alone, but not LMIR3 and LMIR4, as two discrete bands in the lysates of transduced Ba/F3 cells (Fig. 2*B*). However, unlike anti-FLAG Ab, anti-LMIR7 mAb more strongly detected a band with high molecular mass (37 kDa) compared with another band (23 kDa) (Fig. 2*B*), suggesting that anti-LMIR7 mAb reacted preferentially with the glycosylated form of LMIR7 expressed on the cell surface. We then stained hematopoietic cells using anti-LMIR7 mAb. Flow cytometric analysis demonstrated that LMIR7 was not expressed in B cells ($B220^+$) in BM or spleen, in T-lineage cells ($Thy\text{-}1.2^+$ or $CD3^+$) in PB, spleen, or thymus, or in NK cells ($NK1.1^+$) in spleen (Fig. 2, *D* and *E*, and data not shown). On the other hand, immature to mature neutrophils ($CD11b^{high}$) in BM or mature neutrophils ($CD11b^{high}$) in PB were $LMIR7^{dull/low}$, and monocytes ($Ly6c^{high}$) in PB were $LMIR7^{high}$ (Fig. 2*D*). Interestingly, a population of $CD11c^+$ cells in PB, but not in spleen, were $LMIR7^{high}$ (Fig. 2*D* and data not shown). Notably, peritoneal macrophages ($F4/80^+$) displayed high expression levels of

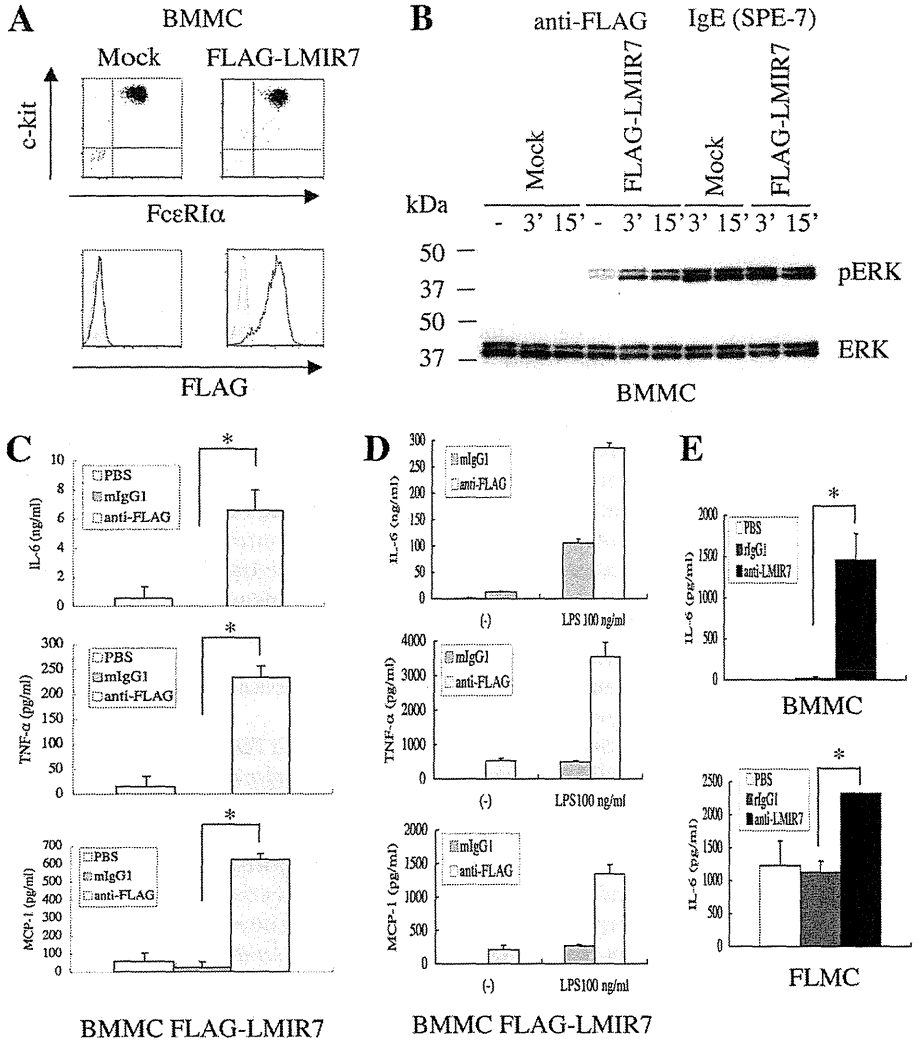

FIGURE 3. **Cross-linking of LMIR7 induced the phosphorylation of ERK in mast cells, resulting in cytokine/chemokine production.** *A*, the surface expression levels of c-Kit and FcεRIα in BMMC expressing FLAG-tagged LMIR7 or mock were analyzed by flow cytometry (*upper panel*). Cells were stained with FITC-conjugated anti-FLAG mAb (*lower panel*) as described. *B*, BMMC expressing FLAG-tagged LMIR7 or mock were stimulated with 10 μg/ml anti-FLAG mAb or 10 μg/ml IgE for 3 or 15 min as indicated. Cell lysates were subject to immunoblotting with anti-phospho-p44/42 MAPK (pERK1/2) Ab. The immunoblots were reprobed with Ab specific for ERK1/2. *C–E*, IL-6, TNF-α, and MCP-1 released into the culture supernatants were measured by ELISA. All data points correspond to the mean ± S.D. of three independent experiments. Statistically significant differences are shown. *, $p < 0.05$. *C*, BMMC expressing FLAG-tagged LMIR7 or mock were stimulated with anti-FLAG Ab, mouse IgG_1, or PBS for 24 h as described under "Experimental Procedures." *D*, BMMC expressing FLAG-tagged LMIR7 or mock were stimulated with anti-FLAG Ab or mouse IgG_1 in the presence or absence of 100 ng/ml LPS as described under "Experimental Procedures." *E*, BMMC (*upper panel*) or FLMC (*lower panel*) were stimulated with anti-LMIR7 mAb or rat IgG_1 for 24 h as described under "Experimental Procedures."

LMIR7 (Fig. 2*D*). When BMMC, BMmDC, BMpDC, and BMMΦ were stained with anti-LMIR7 mAb, we found that BMmDC and BMpDC expressed scarcely detectable levels of LMIR7 (Fig. 2*E*). Remarkably, LMIR7 was expressed at high levels in BMMC as well as in BMMΦ (Fig. 2*E*). Taken together with the results on LMIR7 expression at transcript levels, these findings indicated that LMIR7 was not expressed in lymphoid-lineage cells, except for a few B-lineage cell lines, but was broadly expressed in myeloid-lineage cells. Importantly, LMIR7 was highly expressed in mast cells, monocytes/macrophages, and a small subset of $CD11c^+$ cells in PB. High expression levels of endogenous LMIR7 in BMMC and BMMΦ were also confirmed by Western blot analysis (Fig. 2*C*). Because LMIR4 is predominantly expressed in neutrophils, the present results indicated that LMIR7 and LMIR4 were differentially distributed in hematopoietic cells.

LMIR7 Engagement Induced the Activation of BMMC—In view of expression profiles of LMIR7, we examined the functions of LMIR7 in mast cells. BMMCs were retrovirally transduced with either FLAG-tagged LMIR7 or mock. We found comparable expression levels of c-Kit and FcεRI in both BMMCs and confirmed the expression of transduced LMIR7 by staining with anti-FLAG mAb (Fig. 3*A*). In addition, transduction with LMIR7 did not affect the differentiation or the growth of BMMCs (data not shown). Although stimulation with IgE induced equivalent levels of ERK phosphorylation in both BMMCs, stimulation with anti-FLAG mAb led to ERK activation only in LMIR7-transduced BMMCs (Fig. 3*B*). Accordingly, stimulation with anti-FLAG mAb-loaded beads resulted in robust cytokine/chemokine (IL-6, TNF-α, and MCP-1) production of BMMCs expressing FLAG-LMIR7 (Fig. 3*C*). We confirmed that stimulation with control Ab-coated beads did not induce significant levels of cytokine/chemokine production in these cells (Fig. 3*C*). On the other hand, a similar stimulation did not cause degranulation, characterized by β-hexosaminidase release, of the LMIR7-transduced BMMCs (data not shown). Interestingly, cross-linking of LMIR7 synergistically enhanced the cytokine/chemokine production of LMIR7-transduced BMMC stimulated by LPS through TLR4 (Fig. 3*D*). Importantly, BMMC or FLMC produced significant levels of IL-6 when endogenous LMIR7 was engaged with anti-LMIR7 mAb-loaded beads but not control Ab-loaded beads (Fig. 3*E*). Collectively, our results show that LMIR7 cross-linking alone induced the activation of mast cells leading to cytokine/chemokine production, demonstrating that LMIR7 is an activating receptor.

FcRγ Deficiency Did Not Affect Surface Expression Levels of LMIR7 in Mast Cells or Macrophages but Dampened Cytokine Production of Mast Cells Stimulated by LMIR7 Cross-linking—LMIR4 transmits an activating signal by interacting with FcRγ

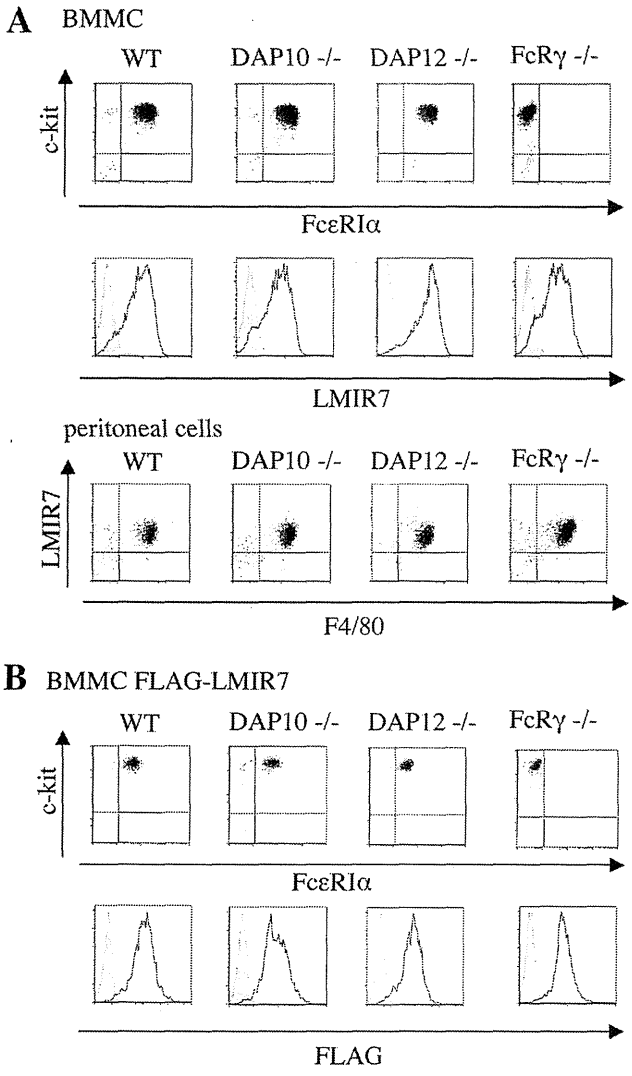

FIGURE 4. **FcRγ is dispensable for surface expression in mast cells or macrophages.** *A*, surface expression levels of endogenous LMIR7 (*middle panel*) or c-Kit and FcεRIα (*top panel*) in BMMC derived from WT, *DAP10*$^{-/-}$, *DAP12*$^{-/-}$, or *FcRγ*$^{-/-}$ mice were analyzed as described in the legend for Fig. 3*A*. Surface expression levels of endogenous LMIR7 and F4/80 (*bottom panel*) in peritoneal cells derived from WT, *DAP10*$^{-/-}$, *DAP12*$^{-/-}$, or *FcRγ*$^{-/-}$ mice were analyzed as described in the legend for Fig. 2*D*. *B*, surface expression levels of FLAG-tagged LMIR7 (*lower panel*) or c-Kit and FcεRIα (*upper panel*) in FLAG-tagged LMIR7-transduced BMMC derived from WT, *DAP10*$^{-/-}$, *DAP12*$^{-/-}$, or *FcRγ*$^{-/-}$ mice were analyzed as described.

among adaptor molecules containing ITAM or the related activating motif-bearing molecules (2). We asked which adaptor molecule plays an important role in LMIR7-mediated activating signal. Flow cytometric analysis demonstrated that surface expression levels of LMIR7 did not differ among wild type (WT) and DAP10, DAP12, or FcRγ-deficient peritoneal MΦ or BMMC (Fig. 4*A*). We confirmed that surface expression levels of FcεRI and c-Kit among these BMMCs were comparable and that those of FcεRI in FcRγ-deficient BMMC were not detectable (Fig. 4*A*), as reported (2, 16). In addition, neither DAP10/DAP12 nor DAP12/FcRγ double deficiency affected surface expression levels of LMIR7 (data not shown). Moreover, when LMIR7 was transduced into DAP10-, DAP12-, or FcRγ-deficient or WT BMMC, the surface expression levels of transduced LMIR7 as well as FcεRI and c-Kit were comparable among these transfectants (Fig. 4*B*). We confirmed that FcεRI expression was not detectable in FcRγ-deficient BMMC (Fig. 4*B*) as reported (16). Taken together, these results indicated that DAP10, DAP12, or FcRγ did not affect surface expression levels of LMIR7. To examine whether adaptor molecules are involved in LMIR7 functions, we stimulated these transfectants with anti-FLAG mAb- or control mAb-loaded beads. Strikingly, LMIR7-mediated cytokine production was abolished by a deficiency in FcRγ but not DAP10 or DAP12, although we found comparable levels of cytokine production among these cells stimulated using phorbol 12-myristate 13-acetate as control (Fig. 5*A*). Consistently, ERK activation of LMIR7-transduced BMMC stimulated by LMIR7 cross-linking, but not by SCF as control, was absent in FcRγ-deficient cells (Fig. 5*B*). We then asked whether LMIR7 physically associated with FcRγ. To this end, 293T cells were co-transfected with FcRγ or a control construct together with a FLAG-tagged LMIR7 or a control construct. Co-immunoprecipitation experiments demonstrated that FcRγ interacted significantly with LMIR7 (Fig. 5*C*). Collectively, these results indicated that FcRγ was required for LMIR7-mediated activation signaling but was dispensable for surface expression of LMIR7.

Strong Interaction of LMIR4 with FcRγ in Comparison with LMIR7 Depended on the Extracellular Juxtamembrane Region and the Transmembrane Domain of LMIR4—In the course of this study, we found that FcRγ were less efficiently co-immunoprecipitated with LMIR7 in comparison with LMIR4 (Fig. 6*C* and data not shown). We next sought to dermine the molecular mechanism by which LMIR4-FcRγ interaction becomes stronger than LMIR7-FcRγ interaction. As shown in Fig. 6*A*, LMIR7 differed from LMIR4 by only three amino acid residues in the transmembrane domain. As it is generally accepted that a transmembrane structure plays a critical role in receptor interaction (15, 24, 25), we generated a chimera receptor composed of an extracellular domain, LMIR7, a transmembrane domain, LMIR4, and an intracellular domain, LMIR7, designated LMIR7-M1. When Ba/F3 cells were transduced with Myc-tagged LMIR-M1 as well as Myc-tagged LMIR4, LMIR7, or mock, flow cytometric analysis using anti-Myc mAb showed that surface expression levels of LMIR7-M1 were equivalent to those of LMIR4 and lower than those of LMIR7 (Fig. 6*B*). These results indicated that the transmembrane domain of LMIR7 was indispensable for maintaining surface expression of LMIR7 at high levels. Interestingly, further transduction with FcRγ into these Ba/F3 cells weakly or moderately increased the surface expression levels of LMIR7-M1 or LMIR4, respectively, although it did not affect those of LMIR7 (Fig. 6*B*). We also performed co-immunoprecipitation experiments similar to those described in Fig. 5*C*. Notably, FcRγ was efficiently co-immunoprecipitated with LMIR7-M1 in comparison with LMIR7, whereas the amount of FcRγ co-immunoprecipitated with LMIR7-M1 was still lower than that co-immunoprecipitated with LMIR4 (Fig. 6*C*). These results led us to ask whether a structural domain other than the transmembrane domain of LMIR4 was involved in the tight interaction between LMIR4 and

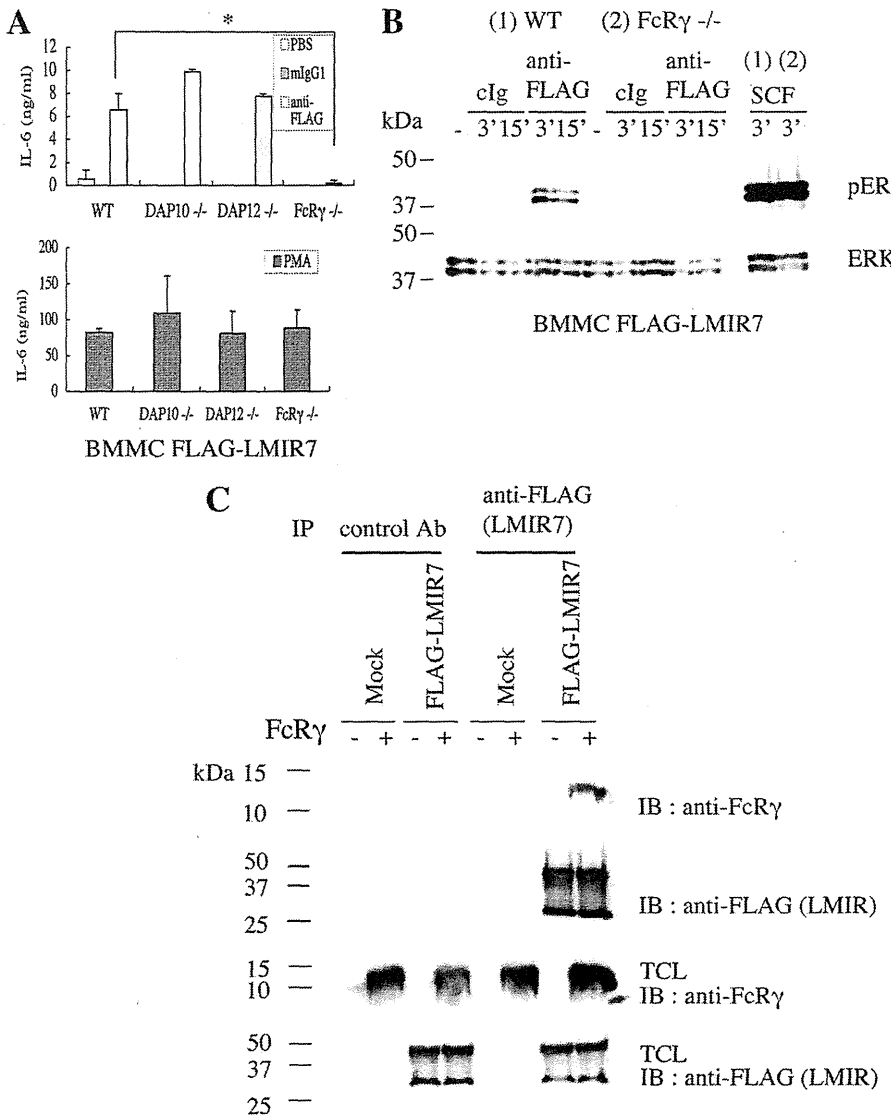

FIGURE 5. **FcRγ is required for LMIR7-mediated activation of mast cells.** *A*, IL-6 released into the culture supernatants was measured by ELISA. WT, *DAP10*$^{-/-}$, *DAP12*$^{-/-}$, or *FcRγ*$^{-/-}$ BMMC expressing FLAG-tagged LMIR7 were stimulated with anti-FLAG mAb, mouse IgG_1, or PBS (*upper panel*) or 50 nM phorbol 12-myristate 13-acetate (*PMA*, *lower panel*) for 24 h as described under "Experimental Procedures." All data points correspond to the mean ± S.D. of three independent experiments. Statistically significant differences are shown. *, $p < 0.05$. *B*, WT or *FcRγ*$^{-/-}$ BMMC expressing FLAG-tagged LMIR7 were stimulated with 10 μg/ml anti-FLAG Ab or mouse IgG_1 or 50 ng/ml SCF for the indicated time. Cell lysates were subject to immunoblotting with anti-phospho-p44/42 MAPK (pERK1/2) Ab. The immunoblots were reprobed with Ab specific for ERK1/2. *C*, 293T cells were transiently co-transfected with a FLAG-tagged LMIR7 or mock and an FcRγ construct or mock. Immunoprecipitates of lysates of these transfectants with anti-FLAG mAb were probed with polyclonal anti-FcRγ Ab or anti-FLAG mAb. One representative of three independent experiments is shown. *IB* and *IP* indicate immunoblot and immunoprecipitation, respectively. *TCL* indicates total cell lysates.

FcRγ. We paid attention to the difference of six amino acid residues (SRPHTR *versus* NSLFIW) in the extracellular juxtamembrane domain of LMIR4 *versus* LMIR7 (Fig. 6*A*). We additionally generated two types of chimera receptors: LMIR7-M2, where an extracellular juxtamembrane region of LMIR7 was replaced with that of LMIR4, and LMIR7-M3, where both an extracellular juxtamembrane region and a transmembrane domain were replaced with those of LMIR4 (Fig. 6*A*). Myc-tagged LMIR7-M2 or LMIR7-M3 was transduced into Ba/F3 cells, demonstrating that surface expression levels of LMIR7-M2 were higher than those of LMIR7 and that surface expression levels of LMIR7-M3 were lower and higher than those of LMIR-M2 and LMIR-M1, respectively (Fig. 6*B*). On the other hand, the presence of FcRγ weakly or moderately increased the surface expression levels of LMIR7-M2 or LMIR7-M3, respectively (Fig. 6*B*). Intriguingly, the amount of FcRγ co-immunoprecipitated with LMIR7-M2 or LMIR7-M3 was comparable with that co-immunoprecipitated with LMIR7-M1 or LMIR4, respectively (Fig. 6*C*). Collectively, these results indicated that the extracellular juxtamembrane region of LMIR4 had a positive effect on its surface expression levels, whereas the transmembrane domain of LMIR4 had a negative effect. In addition, the extracellular juxtamembrane region as well as the transmembrane domain of LMIR4 played a critical role in the strong interaction between LMIR4 and FcRγ. For further analysis, we generated two chimeric receptors: LMIR4-M1, where the transmembrane domain of LMIR4 was replaced with that of LMIR7, and LMIR4-M2, where the extracellular juxtamembrane region was replaced with that of LMIR7 (Fig. 6*A*). Myc-tagged LMIR4-M1 or LMIR4-M2 was transduced into Ba/F3 cells, demonstrating that surface expression levels of LMIR4-M1 or LMIR4-M2 were higher or lower, respectively, than those of LMIR4 (Fig. 6*D*). These results indicated the negative effect of the extracellular juxtamembrane region of LMIR7 on its surface expression levels, as well as the positive effect of the transmembrane domain of LMIR7. The presence of FcRγ did not significantly increase the surface expression levels of LMIR4-M1 or LMIR4-M2 (Fig. 6*D*). We found that FcRγ co-immunoprecipitated with LMIR4-M1 or LMIR4-M2, but the amount of FcRγ co-immunoprecipitated with LMIR4-M1 or LMIR4-M2 was lower than that co-immunoprecipitated with LMIR4 (Fig. 6*E*). It should be noted that the amount of FcRγ co-immunoprecipitated with LMIR4-M1 was lower than that co-immunoprecipitated with LMIR4-M2, notwithstanding the higher expression levels of LMIR4-M1 in comparison with LMIR4-M2 (Fig. 6*E*). Taken together, these results suggested that both the transmembrane domain and the extracellular juxtamembrane

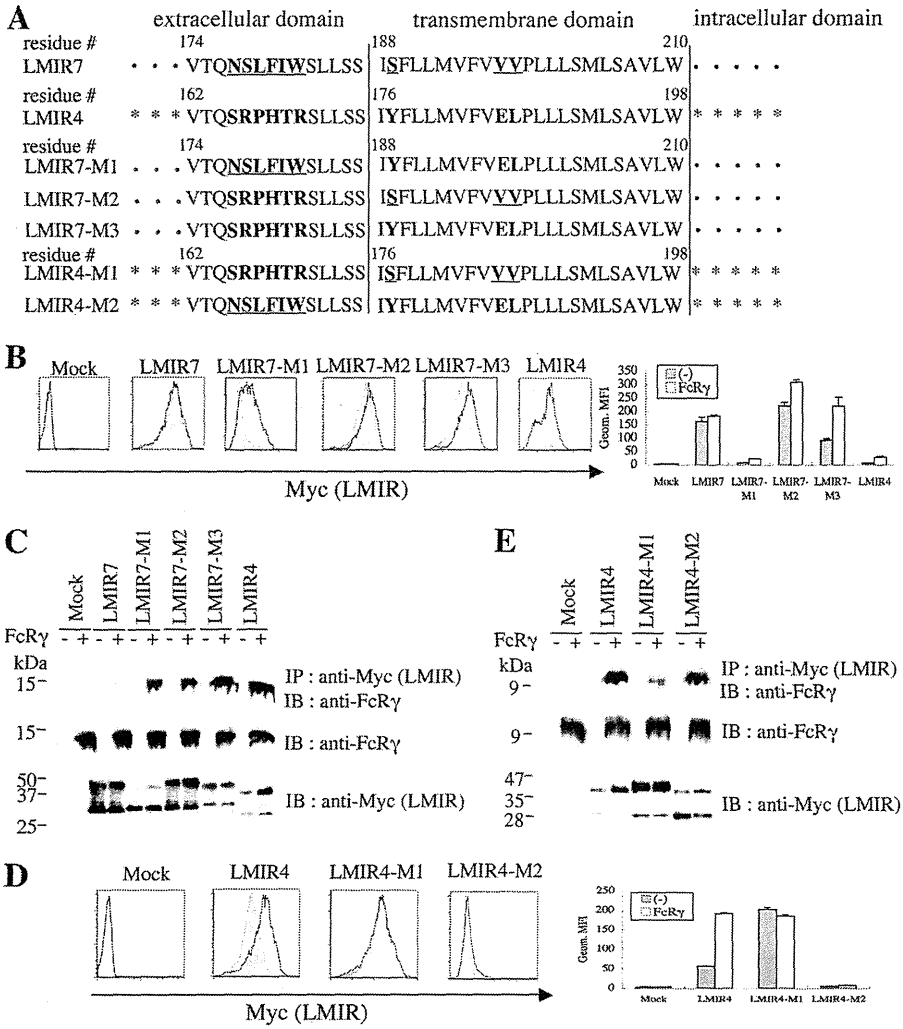

FIGURE 6. **Both the extracellular juxtamembrane region and the transmembrane domain of LMIR4 are indispensable for stronger association of LMIR4-FcRγ as compared with LMIR7-FcRγ.** *A*, alignment of amino acid sequences of the extracellular juxtamembrane and transmembrane domains in LMIR4, LMIR7, and chimera receptors (LMIR7-M1, LMIR7-M2, LMIR7-M3, LMIR4-M1, and LMIR4-M2) are shown using SMART (simple modular architecture research tool) software. Different amino acid residues between LMIR4/CLM-5 (GenBank™ accession number AY457051) and LMIR7/CLM-3 (GenBank™ accession number AY457049) in extracellular juxtamembrane and transmembrane domains are shown in *boldface*, and among these LMIR7-specific amino acid residues are *underlined*. A dot (·) or an asterisk (*) indicates an amino acid residue of the extracellular and intracellular domains of LMIR7 or LMIR4, respectively. *B*, Ba/F3 cells were transduced with (Myc-tagged LMIR7, LMIR7-M1, LMIR7-M2, LMIR7-M3, LMIR4, or mock) plus (FcRγ or alone). Cells were stained with FITC-conjugated anti-Myc mAb. The results of staining (*left panel*) are shown as a *filled histogram* (Ba/F3 cells without FcRγ) or *bold line histogram* (Ba/F3 cells expressing FcRγ). The geometric mean fluorescence intensities (*Geom. MFI*) of Myc-tagged receptors were measured by flow cytometry (*right panel*). All data points correspond to the mean ± S.D. of three independent experiments. One representative of three independent experiments is shown. *C*, 293T cells were transiently co-transfected with (a Myc-tagged LMIR7, LMIR7-M1, LMIR7-M2, LMIR7-M3, LMIR4, or mock) and (an FcRγ construct or alone). Immunoprecipitates of the lysates of these transfectants with anti-Myc mAb were probed with anti-FcRγ Ab. Total cell lysates of these transfectants were also immunoblotted with anti-FcRγ Ab or anti-Myc mAb. One representative of three independent experiments is shown. *IB* and *IP* indicate immunoblot and immunoprecipitation, respectively. *D*, Ba/F3 cells were transduced with (Myc-tagged LMIR4, LMIR4-M1, LMIR4-M2, or mock) plus (FcRγ or mock). Cells were stained with anti-Myc mAb or mouse IgG_1 as control followed by PE-conjugated anti-mouse IgG goat $F(ab')_2$ Ab. The results of staining (*left panel*) are shown as a *filled histogram* (Ba/F3 cells without FcRγ) or *bold line histogram* (Ba/F3 cells expressing FcRγ). The geometric mean fluorescence intensities of Myc-tagged receptors were measured by flow cytometry (*right panel*). All data points correspond to the mean ± S.D. of three independent experiments. One representative of three independent experiments is shown. *E*, 293T cells were transiently co-transfected with (a Myc-tagged LMIR4, LMIR4-M1, LMIR4-M2, or mock) and (an FcRγ construct or alone). Immunoprecipitates of lysates of these transfectants with anti-Myc mAb were probed with anti-FcRγ Ab. Total cell lysates of these transfectants were also immunoblotted with anti-FcRγ Ab or anti-Myc mAb. One representative of three independent experiments is shown.

region of LMIR4 were required, but in different ways, for the efficient up-regulation of surface LMIR4 by the LMIR4-FcRγ interaction.

DISCUSSION

In the present study, we have characterized LMIR7 as an activating receptor closely related to LMIR4 among the LMIR family receptors. Homology research has indicated that LMIR7 is similar to LMIR4 in structure: between them, 85% of the Ig-like domain and 87% of the transmembrane domain are identical in amino acid sequences. Interestingly, neither LMIR7 nor LMIR4 possesses a positively charged residue in the transmembrane domain that is thought to be required for the interaction with ITAM or related activating motif-bearing adaptor proteins. However, our conclusion that, like LMIR4, LMIR7 interacts with FcRγ and thereby transmits an activating signal is based on the following findings: cross-linking of LMIR7 induces ERK activation and cytokine production in BMMC; these activation events are dampened by FcRγ deficiency; and FcRγ is co-immunoprecipitated with LMIR7.

Notably, despite the high homology of the transmembrane domains, several differences exist between LMIR7 and LMIR4. LMIR7-FcRγ interaction is weaker than LMIR4-FcRγ interaction; surface expression levels of LMIR7 are higher than those of LMIR4 (Fig. 6). Our analysis of chimera receptors delineated the relevant molecular mechanism. The transmembrane domain of LMIR7 played a role in maintaining its surface expression at high levels, and probably no charged residue in the transmembrane domain stabilized LMIR7 on the cell surface even in the absence of FcRγ. Interestingly, the extracellular juxtamembrane region of LMIR7 had a negative effect on its surface expression levels, whereas that of LMIR4 had a positive effect. We also reasoned that FcRγ expression did not further increase the surface expression of LMIR7, presumably because of the

weak interaction of LMIR7 with FcRγ. In addition, the weak but significant levels of LMIR7-FcRγ interaction might be explained by a leucine zipper-like interaction between the transmembrane region of LMIR7 and FcRγ. As reported (25), a leucine zipper-like interaction formed by FcRγ residues (Leu-14 and Leu-21) and FcαRI residues (Leu-217, Leu-220, and Leu-224) as well as an Arg/Asp charge interaction formed by the FcRγ residue (Asp-11) and the FcαRI residue (Arg-209) contribute to the tight interaction of both receptors. Interestingly, both LMIR7 and LMIR4 maintain the leucine zipper-like sequences in the transmembrane: LMIR7 residues Leu-202, Leu-205, and Leu-209; and LMIR4 residues Leu-190, Leu-193, and Leu-197. Therefore, it is possible that the leucine zipper-like sequences in the transmembrane of LMIR7 play a role in the LMIR7-FcRγ interaction. In addition, the transmembrane domain of LMIR7 probably contributes to the LMIR7-FcRγ interaction by maintaining surface LMIR7 at high levels. Alternatively, an unknown adaptor molecule might intervene between LMIR7 and FcRγ. Further examination will be necessary to completely understand the precise mechanism of how LMIR7 interacts with FcRγ.

On the other hand, we also speculated that some other mechanism was involved in the strong interaction of LMIR4 with FcRγ. Indeed, we clearly demonstrated by analysis done on chimera receptors that the extracellular juxtamembrane region (amino acid sequence SPRHTR) of LMIR4 played a critical role in the up-regulation of surface LMIR4 by its interaction with FcRγ (Fig. 6). Because there is variability in terms of the expression levels of the chimeric or parent receptors, it is difficult to assess the relative importance of a transmembrane domain *versus* an extracellular juxtamembrane region. However, our results suggested that the transmembrane domain of LMIR4 plays a major role in the high affinity interaction of LMIR4 with FcRγ (Fig. 6*E*). Although the cytoplasmic region, as well as the transmembrane domain, of GPVI is reportedly required for its interaction with FcRγ (23), to our knowledge the present work is the first demonstration that an extracellular juxtamembrane region of an activating receptor plays an important part in the tight interaction with FcRγ. One possibility is that the extracellular juxtamembrane region of LMIR4 interacts with the short extracellular domain of FcRγ. Alternatively, the extracellular juxtamembrane region of LMIR4 might be folded in three-dimensional structure and thereby kept in contact with the transmembrane domain of FcRγ. According to a recent report (24), three polar positions formed by one basic T cell receptor (TCR) α and two ζζ basic aspartic acid transmembrane residues are critical for ζζ dimerization and assembly with T cell receptor. In most cases, this theory is probably valid for activating receptors coupled with FcRγ, considering the high degree of sequence homology between ζ and FcRγ. However, in FcRγ-coupled receptors without a positively charged residue in the transmembrane, the notion presented in this study highlights the novel molecular mechanism of the interaction between activating receptors and FcRγ.

Whereas LMIR4 is expressed predominantly in neutrophils (4), real-time PCR and flow cytometric analysis demonstrated that LMIR7 is highly expressed in mast cells and monocytes/macrophages. Notably, high expression levels of LMIR7 were also observed in an immature subtype of dendritic cell ($CD11c^+$) in PB but not in myeloid or plasmacytoid dendritic cells. Because an inhibitory LMIR3 is broadly expressed in myeloid cells (2, 4), it is likely that LMIR3 pairs with LMIR7 in mast cells and monocytes/macrophages or with LMIR4 in neutrophils. Intriguingly, we showed previously that LMIR3 transmits an inhibitory signal while it interacts with FcRγ and thereby transmits an activating signal in concert with an LPS/TLR4 signal (4). In addition, we demonstrated that like the LMIR4 signal, the LMIR7 signal synergizes with the LPS signal. Therefore, if LMIR3/4/7, with a highly conserved Ig-like domain, had a similar or the same ligand, the LMIR3 signal might inhibit the LMIR7-mediated activating signal or, conversely, cooperate with the LMIR7 signal to enhance the TLR4 signal *in vivo*. In any case, it is possible that LMIR7 or LMIR4 modulates the innate immune responses in a cell type-dependent manner. Complete understanding of the *in vivo* functions of LMIR requires both analysis of each of the knock-out mice and identification of the ligands of each LMIR.

In conclusion, LMIR7 is an activating receptor found among the LMIR family, which transmits an activating signal by interacting with FcRγ. LMIR7 shares similarities with LMIR4 as a counterpart of LMIR3, whereas LMIR7 is regulated differently from LMIR4 in regard to distribution, expression, and function, suggesting a nonredundant role for both activating receptors in other cell types.

Acknowledgments—We thank Dr. Hisashi Arase for providing the pME18S expression vector containing a mouse CD150 leader segment (32). We also thank Dr. Marco Colonna for providing DAP10$^{-/-}$ mice (30). We are grateful to Dr. Dovie Wylie for excellent language assistance.

REFERENCES

1. Kumagai, H., Oki, T., Tamitsu, K., Feng, S. Z., Ono, M., Nakajima, H., Bao, Y. C., Kawakami, Y., Nagayoshi, K., Copeland, N. G., Gilbert, D. J., Jenkins, N. A., Kawakami, T., and Kitamura, T. (2003) *Biochem. Biophys. Res. Commun.* **307,** 719–729
2. Izawa, K., Kitaura, J., Yamanishi, Y., Matsuoka, T., Oki, T., Shibata, F., Kumagai, H., Nakajima, H., Maeda-Yamamoto, M., Hauchins, J. P., Tybulewicz, V. L., Takai, T., and Kitamura, T. (2007) *J. Biol. Chem.* **282,** 17997–18008
3. Yamanishi, Y., Kitaura, J., Izawa, K., Matsuoka, T., Oki, T., Lu, Y., Shibata, F., Yamazaki, S., Kumagai, H., Nakajima, H., Maeda-Yamamoto, M., Tybulewicz, V. L., Takai, T., and Kitamura, T. (2008) *Blood* **111,** 688–698
4. Izawa, K., Kitaura, J., Yamanishi, Y., Matsuoka, T., Kaitani, A., Sugiuchi, M., Takahashi, M., Maehara, A., Enomoto, Y., Oki, T., Takai, T., and Kitamura, T. (2009) *J. Immunol.* **183,** 925–936
5. Chung, D. H., Humphrey, M. B., Nakamura, M. C., Ginzinger, D. G., Seaman, W. E., and Daws, M. R. (2003) *J. Immunol.* **171,** 6541–6548
6. Yotsumoto, K., Okoshi, Y., Shibuya, K., Yamazaki, S., Tahara-Hanaoka, S., Honda, S., Osawa, M., Kuroiwa, A., Matsuda, Y., Tenen, D. G., Iwama, A., Nakauchi, H., and Shibuya, A. (2003) *J. Exp. Med.* **198,** 223–233
7. Luo, K., Zhang, W., Sui, L., Li, N., Zhang, M., Ma, X., Zhang, L., and Cao, X. (2001) *Biochem. Biophys. Res. Commun.* **287,** 35–41
8. Fujimoto, M., Takatsu, H., and Ohno, H. (2006) *Int. Immunol.* **18,** 1499–1508
9. Daish, A., Starling, G. C., McKenzie, J. L., Nimmo, J. C., Jackson, D. G., and Hart, D. N. (1993) *Immunology* **79,** 55–63
10. Bachelet, I., Munitz, A., Moretta, A., Moretta, L., and Levi-Schaffer, F. (2005) *J. Immunol.* **175,** 7989–7995

11. Alvarez-Errico, D., Aguilar, H., Kitzig, F., Brckalo, T., Sayós, J., and López-Botet, M. (2004) *Eur. J. Immunol.* **34,** 3690–3701
12. Ravetch, J. V., and Lanier, L. L. (2000) *Science* **290,** 84–89
13. Takai, T., and Ono, M. (2001) *Immunol. Rev.* **181,** 215–222
14. Colonna, M. (2003) *Nat. Rev. Immunol.* **3,** 445–453
15. Humphrey, M. B., Lanier, L. L., and Nakamura, M. C. (2005) *Immunol. Rev.* **208,** 50–65
16. Takai, T., Li, M., Sylvestre, D., Clynes, R., and Ravetch, J. V. (1994) *Cell* **76,** 519–529
17. Blank, U., Ra, C., Miller, L., White, K., Metzger, H., and Kinet, J. P. (1989) *Nature* **337,** 187–189
18. Scholl, P. R., and Geha, R. S. (1993) *Proc. Natl. Acad. Sci. U.S.A.* **90,** 8847–8850
19. Ra, C., Jouvin, M. H., Blank, U., and Kinet, J. P. (1989) *Nature.* **341,** 752–754
20. Pfefferkorn, L. C., and Yeaman, G. R. (1994) *J. Immunol.* **153,** 3228–3236
21. Morton, H. C., van den Herik-Oudijk, I. E., Vossebeld, P., Snijders, A., Verhoeven, A. J., Capel, P. J., and van de Winkel, J. G. (1995) *J. Biol. Chem.* **270,** 29781–29787
22. Maeda, A., Kurosaki, M., and Kurosaki, T. (1998) *J. Exp. Med.* **188,** 991–995
23. Bori-Sanz, T., Inoue, K. S., Berndt, M. C., Watson, S. P., and Tulasne, D. (2003) *J. Biol. Chem.* **278,** 35914–35922
24. Call, M. E., Schnell, J. R., Xu, C., Lutz, R. A., Chou, J. J., and Wucherpfennig, K. W. (2006) *Cell* **127,** 355–368
25. Wines, B. D., Trist, H. M., Ramsland, P. A., and Hogarth, P. M. (2006) *J. Biol. Chem.* **281,** 17108–17113
26. Kawakami, T., and Galli, S. J. (2002) *Nat. Rev. Immunol.* **2,** 773–786
27. Kraft, S., and Kinet, J. P. (2007) *Nat. Rev. Immunol.* **7,** 365–378
28. Kitaura, J., Song, J., Tsai, M., Asai, K., Maeda-Yamamoto, M., Mocsai, A., Kawakami, Y., Liu, F. T., Lowell, C. A., Barisas, B. G., Galli, S. J., and Kawakami, T. (2003) *Proc. Natl. Acad. Sci. U.S.A.* **100,** 12911–12916
29. Kawakami, T., and Kitaura, J. (2005) *J. Immunol.* **175,** 4167–4173
30. Gilfillan, S., Ho, E. L., Cella, M., Yokoyama, W. M., and Colonna, M. (2002) *Nat. Immunol.* **3,** 1150–1155
31. Kaifu, T., Nakahara, J., Inui, M., Mishima, K., Momiyama, T., Kaji, M., Sugahara, A., Koito, H., Ujike-Asai, A., Nakamura, A., Kanazawa, K., Tan-Takeuchi, K., Iwasaki, K., Yokoyama, W. M., Kudo, A., Fujiwara, M., Asou, H., and Takai, T. (2003) *J. Clin. Invest.* **111,** 323–332
32. Shiratori, I., Ogasawara, K., Saito, T., Lanier, L. L., and Arase, H. (2004) *J. Exp. Med.* **199,** 525–533
33. Kitamura, T., Koshino, Y., Shibata, F., Oki, T., Nakajima, H., Nosaka, T., and Kumagai, H. (2003) *Exp. Hematol.* **31,** 1007–1014
34. Morita, S., Kojima, T., and Kitamura, T. (2000) *Gene Ther.* **7,** 1063–1066
35. Kojima, T., and Kitamura, T. (1999) *Nat. Biotechnol.* **17,** 487–490

Published June 21, 2010

JEM

Article

TIM1 is an endogenous ligand for LMIR5/CD300b: LMIR5 deficiency ameliorates mouse kidney ischemia/reperfusion injury

Yoshinori Yamanishi,[1,3] Jiro Kitaura,[1] Kumi Izawa,[1] Ayako Kaitani,[1] Yukiko Komeno,[1] Masaki Nakamura,[1] Satoshi Yamazaki,[4] Yutaka Enomoto,[1] Toshihiko Oki,[1,2] Hisaya Akiba,[5] Takaya Abe,[6] Tadasuke Komori,[7] Yoshihiro Morikawa,[7] Hiroshi Kiyonari,[6] Toshiyuki Takai,[8] Ko Okumura,[5] and Toshio Kitamura[1,2]

[1]Division of Cellular Therapy and [2]Division of Stem Cell Signaling, The Institute of Medical Science, The University of Tokyo, Minato-ku, Tokyo 108-8639, Japan
[3]Department of Physiological Chemistry and Metabolism, Graduate School of Medicine, The University of Tokyo, Bunkyo-ku, Tokyo 103-0033
[4]Small Animal Model Group, Nakauchi Stem Cell and Organ Regeneration, Japan Science and Technology Agency, Minato-ku, Tokyo 108-8639, Japan
[5]Department of Immunology, Juntendo University School of Medicine, Bunkyo-ku, Tokyo 113-8421, Japan
[6]The Laboratory for Animal Resources and Genetic Engineering, RIKEN Center for Developmental Biology, Kobe 650-0047, Japan
[7]Department of Anatomy and Neurobiology, Wakayama Medical University, Wakayama 641-8509, Japan
[8]Department of Experimental Immunology, Institute of Development, Aging, and Cancer, Tohoku University, Sendai 980-8575, Japan

Leukocyte mono-immunoglobulin (Ig)–like receptor 5 (LMIR5)/CD300b is a DAP12-coupled activating receptor predominantly expressed in myeloid cells. The ligands for LMIR have not been reported. We have identified T cell Ig mucin 1 (TIM1) as a possible ligand for LMIR5 by retrovirus-mediated expression cloning. TIM1 interacted only with LMIR5 among the LMIR family, whereas LMIR5 interacted with TIM4 as well as TIM1. The Ig-like domain of LMIR5 bound to TIM1 in the vicinity of the phosphatidylserine (PS)-binding site within the Ig-like domain of TIM1. Unlike its binding to TIM1 or TIM4, LMIR5 failed to bind to PS. LMIR5 binding did not affect TIM1- or TIM4-mediated phagocytosis of apoptotic cells, and stimulation with TIM1 or TIM4 induced LMIR5-mediated activation of mast cells. Notably, LMIR5 deficiency suppressed TIM1-Fc-induced recruitment of neutrophils in the dorsal air pouch, and LMIR5 deficiency attenuated neutrophil accumulation in a model of ischemia/reperfusion injury in the kidneys in which TIM1 expression is up-regulated. In that model, LMIR5 deficiency resulted in ameliorated tubular necrosis and cast formation in the acute phase. Collectively, our results indicate that TIM1 is an endogenous ligand for LMIR5 and that the TIM1–LMIR5 interaction plays a physiological role in immune regulation by myeloid cells.

CORRESPONDENCE
Toshio Kitamura:
kitamura@ims.u-tokyo.ac.jp

Abbreviations used: BMMC, BM-derived mast cell; CHO, Chinese hamster ovary; ERK, extracellular signal-regulated kinase; FLMC, fetal liver–derived mast cell; IRI, ischemia/reperfusion injury; KIM-1, kidney injury molecule–1; LMIR, leukocyte mono-Ig–like receptor; PS, phosphatidylserine; TIM, T cell Ig mucin.

A growing number of studies have characterized a variety of paired activating and inhibitory receptors (Ravetch and Lanier, 2000; Klesney-Tait et al., 2006; Lanier, 2009). We have previously identified a leukocyte mono-Ig–like receptor (LMIR) mainly expressed in myeloid cells (Kumagai et al., 2003; Izawa et al., 2007; Yamanishi et al., 2008). The mouse LMIR family is also known as the CMRF-35–like molecule/myeloid-associated Ig-like receptor/dendritic cell–derived Ig-like receptor/CD300 family (Luo et al., 2001; Chung et al., 2003; Yotsumoto et al., 2003). LMIR1 and LMIR3 are immunoreceptor tyrosine-based inhibitory motif–containing inhibitory receptors, whereas other members are activating receptors that associate with immunoreceptor tyrosine-based activation motif–containing adaptor proteins (Luo et al., 2001; Chung et al., 2003; Kumagai et al., 2003; Yotsumoto et al., 2003; Izawa et al., 2007; Yamanishi et al., 2008). LMIR5 is a DAP12-coupled activating receptor predominantly expressed in myeloid cells (Yamanishi

The Rockefeller University Press $30.00
J. Exp. Med. Vol. 207 No. 7 1501-1511
www.jem.org/cgi/doi/10.1084/jem.20090581

Supplemental Material can be found at:
http://jem.rupress.org/content/suppl/2010/06/17/jem.20090581.DC1.html

Published June 21, 2010

et al., 2008). However, the ligands for LMIR remained unknown. In this study, we identified T cell Ig mucin 1 (TIM1) as a ligand for LMIR5 by retrovirus-mediated expression cloning (Kitamura et al., 2003).

TIM1–4 are characterized as important regulators of immune responses associated with autoimmunity and allergic diseases (McIntire et al., 2001; Kuchroo et al., 2003, 2008). The TIM molecules are type 1 cell-surface glycoproteins, consisting of an N-terminal IgV domain and a mucin domain. TIM1/hepatitis A virus cellular receptor 1 (Kaplan et al., 1996)/kidney injury molecule–1 (KIM-1; Ichimura et al., 1998) is expressed in activated T cells and delivers a signal that enhances T cell activation and proliferation (Meyers et al., 2005; Umetsu et al., 2005). TIM1 can also interact with itself (Santiago et al., 2007b). In addition, a soluble form of KIM-1/TIM1 is released by shedding (Bailly et al., 2002). On the other hand, TIM4 is expressed in macrophages and dendritic cells and is a natural ligand for TIM1 (Meyers et al., 2005). Interestingly, TIM1 and TIM4 recognize phosphatidylserine (PS) and are critical for the efficient clearance of apoptotic cells (Kobayashi et al., 2007; Miyanishi et al., 2007; Santiago et al., 2007a; Ichimura et al., 2008). Recent reports have demonstrated that the narrow cavity built by the CC' and FG loops of the Ig-like domain is a binding site for PS (Kobayashi et al., 2007; Santiago et al., 2007a,b). In addition, TIM1/KIM-1 expression is strongly induced in the injured kidney epithelial cells (Ichimura et al., 1998, 2008; Waanders et al., 2010), and confers a phagocytic phenotype on epithelial cells (Ichimura et al., 2008). TIM1 is also a marker for renal tubular damage (Waanders et al. 2010).

In the present study, using biological and biochemical analysis, we demonstrate that TIM1 and TIM4 are endogenous ligands for LMIR5. In addition, we generated LMIR5$^{-/-}$ mice and delineated the physiological significance of the LMIR5–TIM1 interaction by using an acute kidney injury model.

RESULTS

Cloning of the ligand for LMIR5

To identify the LMIR5 ligand, we generated an Fc fusion protein containing the extracellular domain of LMIR5 (LMIR5-Fc). Several hematopoietic cell lines were incubated with LMIR5-Fc, which stained A20 cells but not Ba/F3 cells, as determined by flow cytometric analysis, suggesting the expression of LMIR5 ligand in A20 cells (Fig. 1 A). To identify the surface protein bound by LMIR5-Fc, we used retrovirus-mediated expression cloning (Kitamura et al., 2003). A retrovirus cDNA library constructed from A20 cells was transduced via infection to Ba/F3 cells that were not stained by LMIR5-Fc (Fig. 1 A). The transfectants stained by LMIR5-Fc were sorted and expanded in culture. This cycle of sorting and expansion was repeated three times until LMIR5-Fc stained most cells (Fig. S1 A). After we obtained single-cell clones that were stained with LMIR5-Fc, we isolated TIM1 cDNA from most of these clones by PCR (Fig. S1 B and not depicted). We confirmed that a cell-surface glycoprotein TIM1 was expressed in A20 cells but not in Ba/F3 cells by using anti-TIM1 antibody (Fig. 1 A, bottom). When TIM1 was expressed in Ba/F3 cells, LMIR5-Fc strongly stained TIM1-transduced Ba/F3 but not parental Ba/F3 cells. In addition, LMIR5-Fc–staining levels were correlated with TIM1 expression at both surface protein and mRNA levels (Fig. 1, A and B). Collectively, these results indicated that LMIR5-Fc bound to TIM1. In accordance, pretreatment of LMIR5-Fc with 10 μg/ml anti-LMIR5 antibody, but not control antibody, abolished the binding of LMIR5-Fc to TIM1-expressing Ba/F3 cells (Fig. 1 C, left). Similarly, the preincubation of TIM1-expressing Ba/F3 cells with 100 μg/ml anti-TIM1 antibody (222414) suppressed this binding (Fig. 1 D, left). The binding of LMIR5-Fc to TIM1-expressing Ba/F3 cells was dose-dependently inhibited by anti-LMIR5 or anti-TIM1 antibody (Fig. 1, C and D, right). These observations strongly suggested that LMIR5 interacts directly with TIM1. Then, Fc fusion proteins containing the extracellular domains of LMIR1, 2, 3, and 4 (LMIR1/2/3/4-Fc) were generated. TIM1-expressing Ba/F3 cells were bound only by LMIR5-Fc among the LMIR-Fc fusion proteins (Fig. 1 E). When Ba/F3 cells transduced with Flag-tagged TIM1, 2, 3, and 4 were incubated with LMIR5-Fc, LMIR5-Fc bound to those cells transduced with TIM4 as well as TIM1 among the TIM family (Fig. 1 F). In support of this, coimmunoprecipitation experiments illustrated the physical interaction of LMIR5 with both TIM1 and TIM4 (Fig. 1 G). After generating Fc fusion proteins containing the extracellular domains of TIM1 or 4 (TIM1/4-Fc), we incubated LMIR5- or mock-transduced Ba/F3 cells with TIM1-Fc or TIM4-Fc, which stained LMIR5-transduced Ba/F3 cells more strongly as compared with parental Ba/F3 cells (Fig. S1 C), indicating that TIM1 or TIM4 bound to surface-expressed LMIR5. On the other hand, the fact that TIM1-Fc or TIM4-Fc stained parental Ba/F3 cells at significant levels suggested that ligands for TIM1 or TIM4 other than LMIR5 were expressed in Ba/F3 cells. Our results suggested that TIM1 and TIM4 are possible ligands for LMIR5.

The Ig-like domain of LMIR5 binds to that of TIM1 in the vicinity of the PS-binding site

To determine which region of LMIR5 was required for the interaction with TIM1, we generated LMIR5 deletion mutants (LMIR5 del1/2/3/4/5–Fc; Fig. 2, A and B). Notably, like LMIR5-Fc, LMIR5 del1/2/3–Fc bound to TIM1-expressing Ba/F3 cells, whereas LMIR5 del4/5–Fc lacking the C terminus of the Ig-like domains did not bind at all (Fig. 2 C). These results suggested that the intact Ig-like domain of LMIR5 is indispensable for the LMIR5–TIM1 interaction.

According to recent reports, TIM1 and TIM4 bind to PS through the highly conserved binding cleft (FG–CC' cleft) of the Ig-like domains (Kobayashi et al., 2007; Miyanishi et al., 2007; Santiago et al., 2007a,b; Ichimura et al., 2008). To clarify the involvement of this region in LMIR5–TIM1 binding, we generated the TIM1 mutants W115A/F116A (WF/AA) or N117A/D118A (ND/AA), because these mutations in the metal ion–dependent ligand-binding site were reported

Published June 21, 2010

to dampen TIM1–PS binding (Kobayashi et al., 2007; Santiago et al., 2007a). Interestingly, these substitutions completely abolished the binding of LMIR5-Fc to TIM1-expressing Ba/F3 cells (Fig. 2 D). Collectively, these findings indicated that LMIR5 bound to TIM1, presumably through the interaction of the Ig-like domain of LMIR5 with the structural

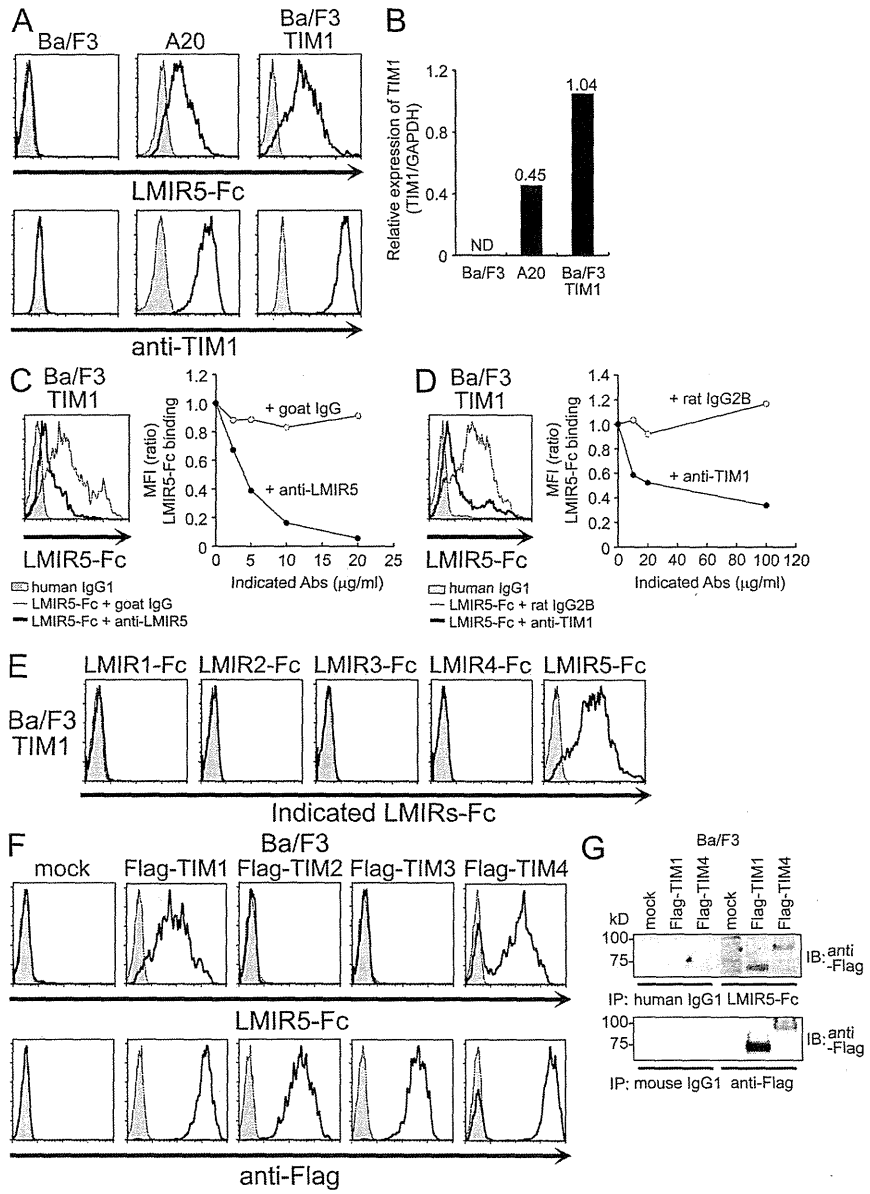

Figure 1. Specific binding of LMIR5-Fc to TIM1-expressing cells. (A) The indicated cells or TIM1-transduced Ba/F3 cells were stained with LMIR5-Fc (top) or with anti-TIM1 antibody (RMT1-4; bottom). (B) Relative gene expression levels of TIM1 were estimated by using real-time PCR. (C) LMIR5-Fc was pretreated with the indicated concentrations (left, 10 μg/ml) of anti-LMIR5 antibody or goat IgG. (D) TIM1-transduced Ba/F3 cells were preincubated with the indicated concentrations (left, 100 μg/ml) of anti-TIM1 antibody (222414) or rat IgG2b. TIM1-transduced Ba/F3 cells were then stained with LMIR5-Fc. The mean fluorescent intensity (MFI) of LMIR5-Fc staining is shown (C and D, right). (E) TIM1-transduced Ba/F3 cells were stained with LMIR1/2/3/4/5-Fc (continuous line histograms). Control staining with human IgG1 is shown (shaded histograms). (F) Ba/F3 cells transduced with Flag-tagged TIM1/2/3/4 or mock transduced were stained with LMIR5-Fc (top, continuous line histograms) or with anti-Flag antibody (bottom, continuous line histograms). Control staining with human (top, shaded histograms) and mouse IgG1 (bottom, shaded histograms) is shown. (G) TIM1 and TIM4 proteins were detected by immunoblotting (IB) with anti-Flag antibody in the immunoprecipitates (IP) of lysates derived from Flag-tagged TIM1-, TIM4-, or mock-transduced Ba/F3 cells incubated with LMIR5-Fc (top) or anti-Flag antibody (bottom). All data are representative of three independent experiments. ND, not detected.

Published June 21, 2010

JEM

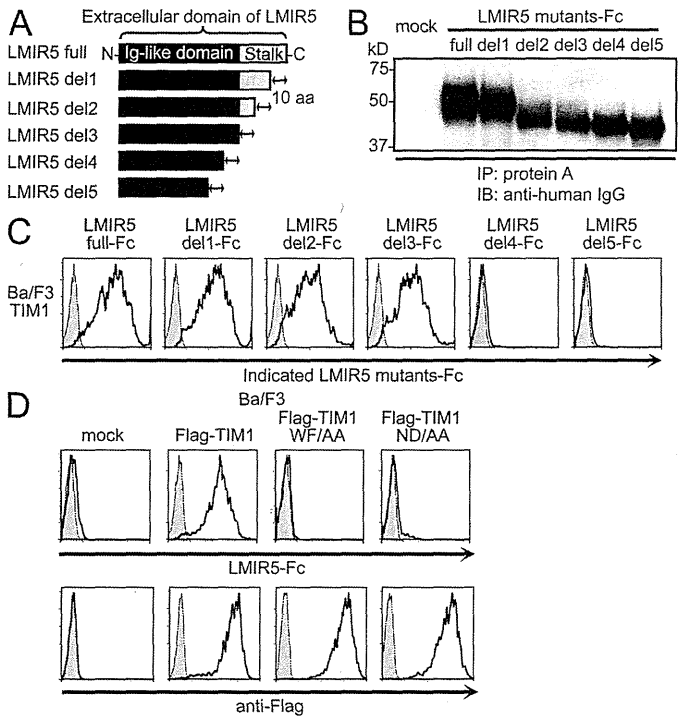

Figure 2. Ig-like domains of both LMIR5 and TIM1 are required for the LMIR5–TIM1 interaction. (A) Structures of LMIR5 extracellular domain in LMIR5-Fc and its deletion mutants. (B) The culture supernatants from 293T cells transduced with LMIR5-Fc or LMIR5-Fc mutants were immunoprecipitated (IP) with protein A, and then immunoblotted (IB) with anti-human IgG antibody. (C) TIM1-transduced Ba/F3 cells were stained with LMIR5-Fc or LMIR5-Fc mutants (continuous line histograms). Control staining with human IgG1 is shown (shaded histograms). (D) Ba/F3 cells transduced with Flag-tagged TIM1, TIM1 (WF/AA), TIM1 (ND/AA), or mock were stained with LMIR5-Fc (top, continuous line histograms) or anti-Flag antibody (bottom, continuous line histograms). Control staining with human (top, shaded histograms) and mouse IgG1 (bottom, shaded histograms) is shown. All data shown are representative of three independent experiments.

domain formed by FG loops of TIM1. Related to this, we found different capabilities of anti-TIM1 antibodies to recognize TIM1 epitopes. Anti-TIM1 antibody (222414) detected TIM1 WT and the ND/AA mutant but not the WF/AA mutant, whereas anti-TIM1 antibody (RMT1-10) detected TIM1 WT and the mutants WF/AA and ND/AA (Fig. S2 A). Thus, anti-TIM1 antibody (222414) presumably recognizes the FG loop structure that is critically maintained by W115/F116 but not N117/D118, whereas anti-TIM1 (RMT1-10) antibody reacts outside this area of TIM1. Then, we compared the inhibitory effect of these antibodies on LMIR5–TIM1 binding. Unlike anti-TIM1 antibody (RMT1-10) or anti-Flag antibody, anti-TIM1 antibody (222414) pretreatment did inhibit LMIR5–TIM1 binding (Fig. S2 B). Collectively, these results suggested that the Ig-like domain of LMIR5 interacted with TIM1 in the region formed by the FG loop of the Ig-like domain, the structure of which was similar or close to the FG–CC' cleft bound by PS, and that it was recognized by anti-TIM1 antibody (222414).

LMIR5 neither binds to PS nor affects TIM1- or TIM4-mediated phagocytosis of apoptotic cells

Given the close proximity of the PS- and LMIR5-binding regions in TIM1, we tested whether LMIR5 interacts with TIM1 through PS. To this end, we performed a protein–lipid overlay assay; although TIM1-Fc bound specifically to PS, as previously reported (Kobayashi et al., 2007; Miyanishi et al., 2007), we found no binding of LMIR5-Fc to PS or to other phospholipids (Fig. 3 A). Consistently, NIH3T3 cells transduced with TIM1 but not LMIR5 promoted phagocytosis of the apoptotic cells through recognition of PS (Fig. 3 B). Next, we asked if the LMIR5–TIM1 interaction affected the TIM1-mediated phagocytosis of the apoptotic cells. As expected, coincubation with anti-TIM1 antibody or TIM1-Fc significantly suppressed phagocytosis of the apoptotic cells in TIM1-expressing NIH3T3 cells (Fig. 3 C). In contrast, coincubation with LMIR5-Fc did not inhibit this phagocytosis (Fig. 3 C). Similarly, the interaction of LMIR5 with TIM4 did not affect TIM4-mediated phagocytosis of the apoptotic cells in peritoneal macrophages (Fig. 3, D and E). Collectively, interaction of neither TIM1 nor TIM4 with LMIR5 affected the phagocytosis of apoptotic cells through its recognition of PS, despite the finding that LMIR5 bound to TIM1 or TIM4 at close proximity to the PS-binding site.

The TIM1–LMIR5 interaction induces LMIR5-mediated activation of mast cells

As previously reported (Kitaura et al., 2003; Yamanishi et al., 2008), LMIR5-mediated activation of mast cells depended on LMIR5 expression levels (Fig. 4 A, left). Notably, stimulation with TIM1-Fc, but not human IgG1 as a control, induced significant levels of extracellular signal-regulated kinase (ERK) activation in LMIR5-transduced BM-derived mast cells (BMMCs), whereas no detectable levels of ERK activation were induced by TIM1-Fc in mock-transduced BMMCs (Fig. 4 A, right). Similarly, stimulation with TIM1-Fc or TIM4-Fc induced cytokine production of fetal liver–derived mast cells (FLMCs) transduced with LMIR5, but not mock-transduced cells (Fig. 4 B; and Fig. S3, A and B). In addition, DAP12 deficiency completely dampened cytokine production of LMIR5-transduced FLMCs stimulated by TIM1-Fc, but not PMA as a control (Fig. 4 B). These results indicated that TIM1-Fc or TIM4-Fc activated mast cells through interaction with LMIR5, which was dependent on the expression levels of LMIR5. As previously reported (Nakae et al., 2007), we found high expression levels of TIM3 as well as

Published June 21, 2010

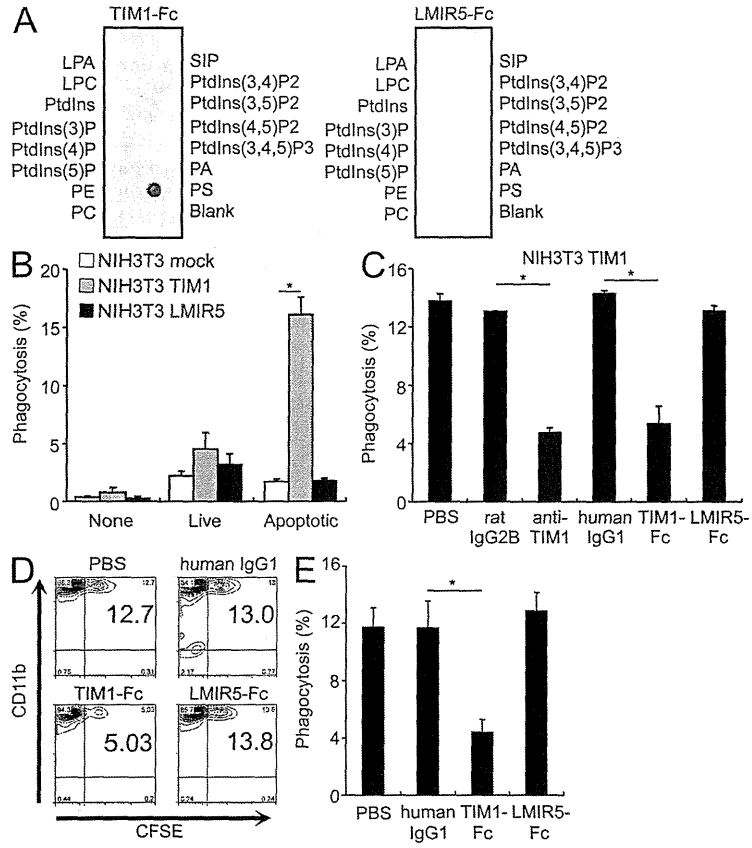

Figure 3. LMIR5 is not involved in TIM1- or TIM4-mediated phagocytosis of apoptotic cells through recognition of PS. (A) PIP strips spotted with the indicated phospholipids were incubated with TIM1-Fc or LMIR5-Fc. (B and C) NIH3T3 cells transduced with either TIM1, LMIR5, or mock were co-cultured with CFSE-labeled live or apoptotic U937 cells in the presence (C) or absence (B) of the indicated antibodies or Fc fusion proteins. The percentage of NIH3T3 cells containing CFSE-labeled U937 cells was determined. (D) Peritoneal macrophages were co-cultured with CFSE-labeled apoptotic thymocytes for 30 min in the presence of 10 µg/ml TIM1-Fc, LMIR5-Fc, or human IgG1. After removal of nonadherent cells, peritoneal macrophages were stained with PE-conjugated anti-CD11b antibody. The percentage of CFSE/CD11b double-positive cells was determined by flow cytometric analysis. (E) Based on the flow cytometric analysis in D, the percentage of phagocytosis is shown. All data points correspond to the means ± SD of triplicate samples. Data are representative of three independent experiments. *, $P < 0.05$.

no detectable expression levels of TIM2 and TIM4 in mast cells (Fig. S4). However, TIM1 expression in mast cells was not confirmed in either protein or transcript levels (Fig. S4). Therefore, we reasoned that the involvement of the TIM1–TIM1/4 interaction in TIM1-Fc–induced activation of mast cells was negligible. We then performed co-culture of LMIR5- or mock-transduced FLMCs with TIM1-transduced Chinese hamster ovary (CHO) cells, demonstrating higher levels of IL-6 released into the supernatants of the former co-culture as compared with the latter (Fig. 4 C, left). In addition, we found higher levels of IL-6 released into the supernatants in the co-culture of LMIR5-expressing FLMCs with TIM1-transduced CHO cells as compared with mock-transduced CHO cells (Fig. 4 C, right). These results indicated that interaction of LMIR5 with surface-expressed TIM1 as well as soluble TIM1 induced the LMIR5-mediated activation of mast cells.

In vivo evidence that the LMIR5–TIM1 interaction induces the accumulation of neutrophils

To investigate the physiological role of TIM1 as a ligand for LMIR5, we generated LMIR5-deficient mice (Fig. S5 A). We confirmed gene targeting by genomic PCR (Fig. S5 B) and the complete absence of LMIR5 expression in BM neutrophils by flow cytometry (Fig. 5 C). Semiquantitative RT-PCR analysis demonstrated no significant difference of LMIR1–4 transcript levels in BM cells between WT and LMIR5$^{-/-}$ mice (Fig. S5 C). LMIR5$^{-/-}$ mice were born at the expected Mendelian ratio and showed no obvious abnormalities. In addition, WT and LMIR5$^{-/-}$ mice did not reveal major differences in the myeloid and lymphoid development of the BM, spleen, thymus, peripheral blood, and peritoneal cells (Fig. S6).

To address the physiological significance of the LMIR5–TIM1 interaction, we chose a model for kidney ischemia/reperfusion injury (IRI; Kelly et al., 1996; Ichimura et al., 1998, 2008; Wu et al., 2007; Lech et al., 2009; Waanders et al., 2010), which is the known in vivo model for TIM1 induction. Consistent with previous reports (Ichimura et al., 1998, 2008; Waanders et al., 2010), TIM1 mRNA levels rapidly increased at day 1 after IRI and diminished through days 2–4 in the IRI kidneys of WT mice, whereas they were maintained at low levels before and after IRI in contralateral kidneys (Fig. 5 A, left). TIM4 mRNA was undetectable in IRI or contralateral kidneys (unpublished data). Notably, LMIR5 mRNA levels increased through days 1 and 2, and thereafter decreased through days 3 and 4 in IRI but not control kidneys of WT mice (Fig. 5 A, right). Further examination showed that in IRI kidneys of WT mice, TIM1 was highly expressed in CD45$^-$ (nonhematopoietic) cells as compared with CD45$^+$ (hematopoietic) cells, whereas LMIR5 was predominantly expressed in CD45$^+$ cells (Fig. 5 B). Together with previous findings (Kelly et al., 1996; Ichimura et al., 1998, 2008; Wu et al., 2007; Lech et al., 2009; Waanders et al., 2010), these results indicated that LMIR5-expressing neutrophils were recruited in IRI kidneys after the up-regulation of TIM1 expression in the renal tubular cells. We then